ISSN 0280-5316
ISRN LUTFD2/TFRT--5788--SE

Trailer Stabilization with AFS

Martin Nilsson

Department of Automatic Control
Lund University
March 2007

Department of Automatic Control
Lund Institute of Technology
Box 118
SE-221 00 Lund Sweden

Document name
MASTER THESIS

Date of issue
March 2007

Document Number
ISRNLUTFD2/TFRT--5788--SE

Author(s)
Martin Nilsson

Supervisor
Christian Lundquist at ZF Lenksysteme in Germany.
Tore Hägglund at Automatic Control in Lund

Sponsoring organization

Title and subtitle
Trailer Stabilization with AFS (Stabilisering av släp med aktiv framhjulsstyrning)

Abstract
People that have driven a car with a trailer at high speed know that the trailer can begin to oscillate. This oscillation is known as snake behavior. How much the car and trailer starts to oscillate depends on how the trailer is loaded. An empty trailer does not tend to oscillate, while a heavy loaded trailer, with the load centered over the trailer axle, oscillates more easily.
For a normal person driving a car and trailer which has started to oscillate, it is not possible to reduce the oscillations in any other way then to lower the speed. A car with AFS (Active Front Steering) can use the steering angle of the front wheels as a counter reaction to the oscillation, and prevent an accident to occur.
For analysis and controller derivation a kinetic model for the car and trailer is derived. Two sorts of controllers are investigated, a linearized model of the system is used to derive a linear controller and linearization feedback with a linear controller. Controlling on the car's yaw rate, the car-trailer angle and the time derivative of the car-trailer angle is tested. Only controlling on the car's yaw rate worked well while controlling the car-trailer angle and it's time derivative did not work, probably because the reference value calculations was not good enough.
The system was implemented in a development car and evaluated at a test track, performing normal driving situations at high speeds. The test results clearly showed that the controller worked as expected, and that almost all oscillations were damped.

Keywords

Classification system and/or index terms (if any)

Supplementary bibliographical information

ISSN and key title
0280-5316

ISBN

Language
English

Number of pages
59

Recipient's notes

Security classification

Acknowledgments

This master's thesis was carried out between July 2006 and December 2006 at ZF Lenksysteme GmbH in Schwäbisch Gmünd, Germany.

I would like to thank all persons who made it possible for me to do this master's thesis. I would like to thank Dr. Wolfgang Reinelt for the correspondence with the university and Christian Lundquist for all the help I received during my work with the thesis. I would also like to thank the people at the department for their help and guidance, Hendrik, Ralf, Frank, Samuel and Martina.

Finally I would like to send my special thanks to my fiancée Jessica, who went with me to Germany, supported me, kept me company during the stay, and for keeping my spirit up during the time I wrote this report.

Lund, February 2007

Contents

Chapter 1

Introduction

In this master's thesis a stabilizing controller for the car-trailer combination is derived and implemented using active steering as actuator. The implemented system is evaluated with respect to the unstable behavior. This is done by test drives at different test tracks.

1.1 Motivation

People driving a car with a trailer have known that the car-trailer combination can give an unstable behavior, which in worst cases can result in an accident. To prevent accidents most car built today have some sort of stabilization control that uses the brakes as actuators (for example ESP, Electronic Stability Program). The company ZF Lenksysteme GmbH has developed a product for BMW called Active Front Steering which can be used as an actuator for stabilization of the car. Interactions from the Active Front Steering are faster then the interactions from the breaks and they are more comfortable, this is why it is more desirable to use the Active Front Steering as actuator instead of the brakes.

1.2 Active Front Steering

The Active Front Steering is an invention which superimposes an electrically controlled angle to the steering wheel angle. The concept can be seen in figure 1.1. The motor angle δ_M is controlled electrical and is summed with the steering wheel angle from the driver δ_S, and together they form the pinion angle δ_G. The pinion angle is mechanically connected to the steering wheel angle δ_F.

1.3 Software and Hardware used in Thesis

For all symbolic calculations the free program Maxima was used. The system was implemented in Matlab Simulink and then compiled to be used in a dSPACE

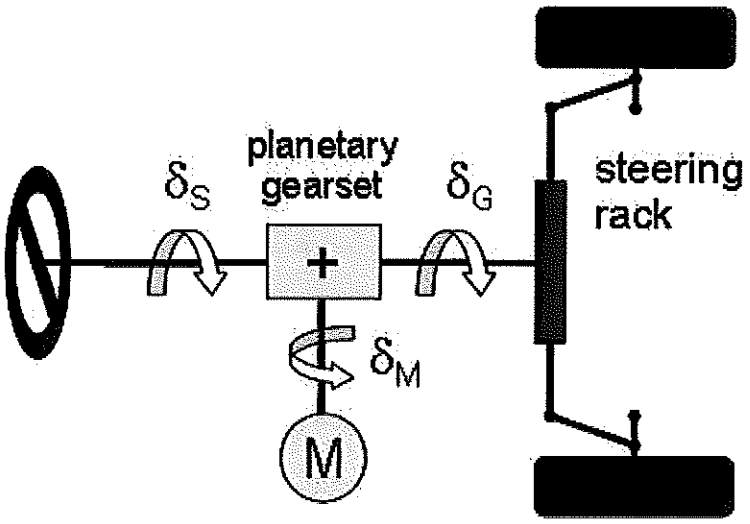

Figure 1.1: The principle of the AFS system. The steering wheel angle δ_S and the electrical controlled motor angle δ_M together gives δ_G.

real time computer that was installed in the car. Parameter optimization was done off line with the help of the Matlab command `lsqnonlin`.

1.4 Notations

The following notation is used.

1.4.1 Acronyms

The following acronyms are used:

AFS	Active Front Steering
DAE	Differential Algebraic Equation
DE	Differential Equation
ESP	Electronic Stability Program
RMSE	Root Mean Square Error

1.4.2 Variables, Constants and Parameters

The following variables, constants and parameters are used in the thesis.

R	reference frame
O	origin of the reference frame
L_i	local frame of body i
P_i	origin of the frame i
Q_i	point i, defined in text
$\boldsymbol{p}$	vector with the coordinates
$\boldsymbol{p}_i$	coordinates for the frame i
$r^R_{P_iO}$	vector from O to P_i seen in frame R
M_i	matrix with mass and moment of inertia of body i
m_i	mass of body i
$J_i^{L_i}$	moment of inertia of body i
f^R_{xi}	force acting along the x-axis of frame R on body i
f^R_{yi}	force acting along the y-axis of frame R on body i
$M_i^{L_i}$	torque acting on body i seen in local frame of body i
f_l	force acting in the longitudinal direction of a tire
f_α	force acting in the lateral direction of a tire
c_α, c_0	cornering stiffness, a tire constant
δ_F	front wheel angle
δ_S	steering wheel angle
δ_G	pinion angle
δ_M	AFS motor angle
β	slip angle of the cars center of mass
α	slip angle of front axle
α_F	slip angle of front wheel/tire
α_R	slip angle of rear wheel
α_T	slip angle of trailer wheel
v	speed of the cars mass center
$\dot{\psi}$	angular velocity of the car
γ	car-trailer angle

Chapter 2

Car and Trailer Model

In this chapter the dynamic model of the car and the trailer is investigated and the differential algebraic equations for the system are derived. First the geometrical definitions of the system are set up, there after the DAEs will be defined. Finally the constraints for the system are derived, making it possible to derive the DEs from the DAEs.

2.1 Basic Geometrical Definitions

The car geometrics can be seen in figure 2.1. Here the global inertial frame R is introduced, this frame can be seen as the fixed road that the car drives on. Further the local frames L_1 and L_2 with their origins located in the mass center of the car respective the mass center of the trailer are shown. For further calculations the displacement vector $r^R_{P_iO} = \begin{pmatrix} x^R_{P_iO} & y^R_{P_iO} \end{pmatrix}^T$ is introduced as seen in figure 2.2. The angle between the frame L_i and the frame R, ψ_i, is defined in figure 2.2. Observe that the angle is positive in counter clockwise

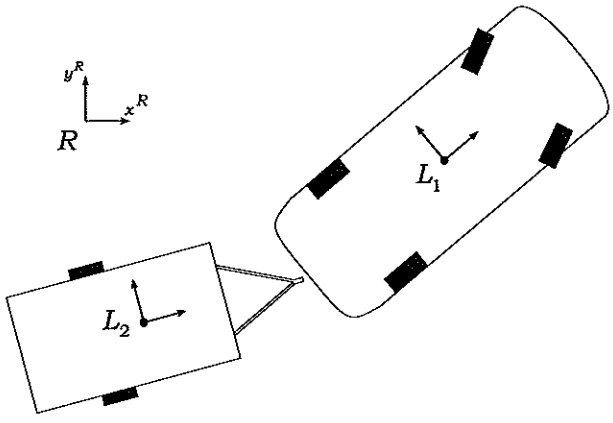

Figure 2.1: Definition of the coordinate system for the car and trailer

rotation.

Define the planar orientation matrix as the matrix that maps a vector represented in L_i into a vector represented in R as

$$A^{RL_i} = \begin{pmatrix} \cos\psi_i & -\sin\psi_i \\ \sin\psi_i & \cos\psi_i \end{pmatrix}. \tag{2.1}$$

The points $Q_1 \ldots Q_5$ and P_1, P_2 are defined according to figure 2.3. Q_1 is the point between the front wheels, Q_2 is the point between the rear wheels, Q_3 is the point at the towing hook of the car, Q_4 is the point of the towing hook on the trailer and Q_5 is the point between the trailer wheels. P_1 is located in the mass center of the car and P_2 is located in the mass center of the trailer.

The car-trailer angle $\gamma = \psi_1 - \psi_2$ is defined as seen in figure 2.4. The γ angle is positive in a left turn.

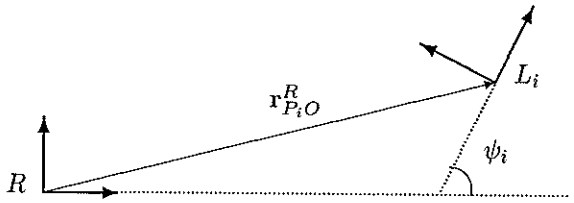

Figure 2.2: Definition of the displacement vector, starting in the origin of frame R and ending in the origin of frame L_i which has the point P_i as the origin.

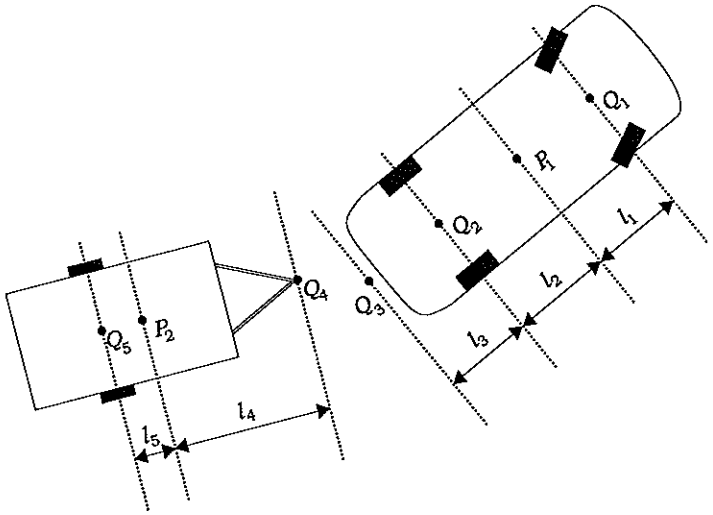

Figure 2.3: Definition of different points on the car and trailer, and the distance between the different points.

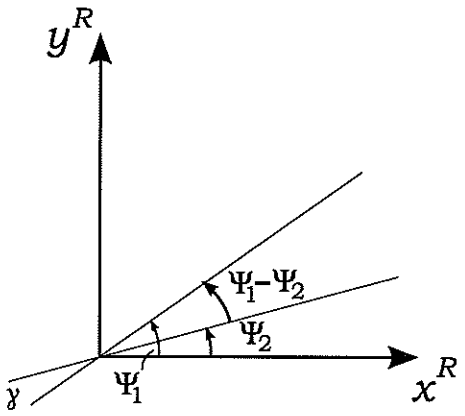

Figure 2.4: Definition of the car-trailer angle gamma

2.2 Bicycle Model

A bicycle model of the car is adopt for the sake of simplicity. Instead of two wheels on each axle of the car and trailer only one wheel is used, in the centerline of the car and trailer. This is shown in figure 2.5.

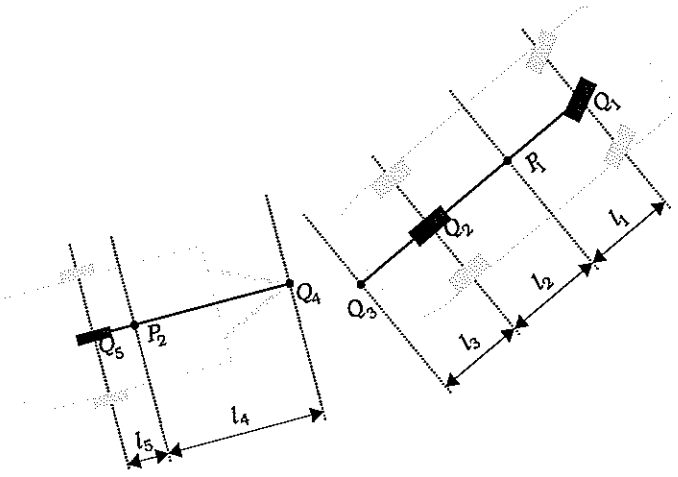

Figure 2.5: Definition of different points on the car and trailer using a bicycle model.

2.3 The Differential Algebraic Equations

In small mechanisms with few bodies and few forces acting on the bodies it is often simple and straight forward to derive the DEs. The car and trailer system includes a large number of forces and a passive joint connecting the two bodies

which makes this a complex system. Therefore the theory of modeling bodies with constraints described in [1] is applied.

2.3.1 General Equations

Each body's position is described with three coordinates that are gathered in the position vector $\boldsymbol{p}_i$ according to

$$\boldsymbol{p}_i = \begin{pmatrix} x^R_{P_iO} & y^R_{P_iO} & \psi_i \end{pmatrix}^T. \tag{2.2}$$

Each body's position vector is gathered in the system position vector $\boldsymbol{p}$ with the definition

$$\boldsymbol{p} = \begin{pmatrix} \boldsymbol{p}_1^T & \boldsymbol{p}_2^T \end{pmatrix}^T. \tag{2.3}$$

The whole system position is described by the 6 elements in $\boldsymbol{p}$. The time derivative of $\boldsymbol{p}$ is defined as

$$\dot{\boldsymbol{p}} = \begin{pmatrix} \dot{\boldsymbol{p}}_1^T & \dot{\boldsymbol{p}}_2^T \end{pmatrix}^T \tag{2.4}$$

where

$$\dot{\boldsymbol{p}}_i = \begin{pmatrix} \dot{x}^R_{P_iO} & \dot{y}^R_{P_iO} & \dot{\psi}_i \end{pmatrix}^T. \tag{2.5}$$

The velocity vector and the time derivative of the position vector has in this planar case the relation

$$\boldsymbol{v} = \dot{\boldsymbol{p}}. \tag{2.6}$$

The mass matrix is defined as

$$M = \text{diag}\,(M_1\ M_2) \tag{2.7}$$

with

$$M_i = \text{diag}\,(m_i\ m_i\ J_i^{L_i}) \tag{2.8}$$

where m_i is the mass of body i and $J_i^{L_i}$ is the moment of inertia for the body i. The matrix

$$q_G = 0 \tag{2.9}$$

because both local frames have their origins in the center of mass of their respectively body.

2.3.2 Forces Acting on the System

The force vector is defined as

$$\boldsymbol{f} = \begin{pmatrix} \boldsymbol{f}_1^T & \boldsymbol{f}_2^T \end{pmatrix}^T \tag{2.10}$$

with

$$\boldsymbol{f}_i^T = \begin{pmatrix} \sum f^R_{xi} \\ \sum f^R_{yi} \\ \sum M_i^{L_i} \end{pmatrix}. \tag{2.11}$$

$\sum f_{xi}^R$ and $\sum f_{yi}^R$ are the sums of forces acting on body i seen in the frame R and $\sum M_i^{L_i}$ is the sum of torque acting on body i seen in the frame L_i.

The forces acting on the car are defined in figure 2.6. From these definitions the following force vector elements are derived.

$$\begin{pmatrix} \sum f_{x1}^R \\ \\ \sum f_{y1}^R \end{pmatrix} = \begin{pmatrix} f_{lF} \cdot (\cos\delta_F \cdot \cos\psi_1 - \sin\delta_F \cdot \sin\psi_1) \\ +f_{\alpha f} \cdot (-\cos\delta_F \cdot \sin\psi_1 - \sin\delta_F \cdot \cos\psi_1) \\ +f_{lR} \cdot \cos\psi_1 - f_{\alpha R} \sin\psi_1 \\ \\ f_{lF} \cdot (\cos\delta_F \cdot \sin\psi_1 + \sin\delta_F \cdot \cos\psi_1) \\ +f_{\alpha f} \cdot (\cos\delta_F \cdot \cos\psi_1 - \sin\delta_F \cdot \sin\psi_1) \\ +f_{lR} \cdot \sin\psi_1 + f_{\alpha R} \cos\psi_1 \end{pmatrix} \tag{2.12}$$

$$= \begin{pmatrix} f_{lF} \cdot \cos(\delta_F + \psi_1) - f_{\alpha f} \cdot \sin(\delta_F + \psi_1) \\ +f_{lR} \cdot \cos\psi_1 - f_{\alpha R} \sin\psi_1 \\ \\ f_{lF} \cdot \sin(\delta_F + \psi_1) + f_{\alpha f} \cdot \cos(\delta_F + \psi_1) \\ +f_{lR} \cdot \sin\psi_1 + f_{\alpha R} \cos\psi_1 \end{pmatrix}. \tag{2.13}$$

From the definitions of forces acting on the trailer in figure 2.7 the following force vector components are derived.

$$\begin{pmatrix} \sum f_{x2}^R \\ \\ \sum f_{y2}^R \end{pmatrix} = \begin{pmatrix} f_{lT} \cdot \cos\psi_2 - f_{\alpha T} \sin\psi_2 \\ \\ f_{lT} \cdot \sin\psi_2 + f_{\alpha T} \cos\psi_2 \end{pmatrix}. \tag{2.14}$$

For the torque element in the force matrix there is the comfortable relationship that $\mathbf{M} = \mathbf{r} \times \mathbf{F}$ giving

$$\sum M_1^{L_1} = l_1 \cdot (\cos\delta_F \cdot F_{\alpha F} + \sin\delta_F \cdot F_{lF}) - l_2 \cdot F_{\alpha R} \tag{2.15}$$

$$\sum M_2^{L_2} = -l_5 \cdot F_{\alpha T}. \tag{2.16}$$

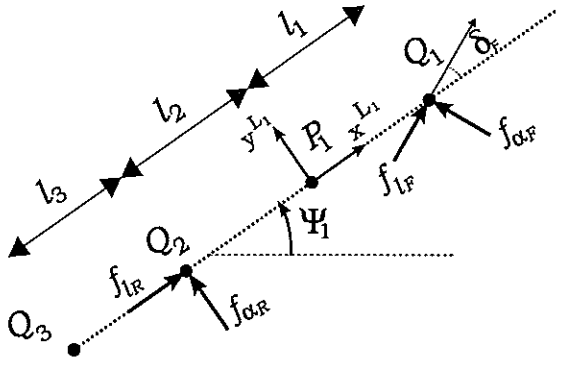

Figure 2.6: Definition of forces acting on car. f_l represents a longitudinal force where as f_α represents a lateral force. Q_1 and Q_2 is the front and rear wheel respectively.

2.4 Constraint Equations

The two bodies are connected through the trailer hook, meaning that there exists a constraint for how the bodies can move in relation to each other. The trailer hook is modeled as a revolutional joint.

The two point coinciding are Q_3 for the car and Q_4 for the trailer. This leads to the constraint position equation

$$r^R_{P_1O} + r^R_{Q_3P_1} - (r^R_{P_2O} + r^R_{Q_4P_2}) = 0 \tag{2.17}$$

or

$$r^R_{P_1O} + \mathbf{A}^{RL_1} \cdot r^{L_1}_{Q_3P_1} - (\mathbf{A}^{RL_2} \cdot r^{L_2}_{Q_4P_2} + r^R_{P_2O}) = 0 \tag{2.18}$$

where

$$r^{L_1}_{Q_3P_1} = \begin{pmatrix} -(l_3 + l_2) \\ 0 \end{pmatrix} \tag{2.19a}$$

$$r^{L_2}_{Q_4P_2} = \begin{pmatrix} l_4 \\ 0 \end{pmatrix}. \tag{2.19b}$$

All together gives

$$\begin{array}{rcl} x^R_{P_1O} - (l_3 + l_2) \cdot \cos\psi_1 - l_4 \cdot \cos\psi_2 - x^R_{P_2O} &=& 0 \\ y^R_{P_1O} - (l_3 + l_2) \cdot \sin\psi_1 - l_4 \cdot \sin\psi_2 - y^R_{P_2O} &=& 0. \end{array} \tag{2.20}$$

With this all matrices needed to set up the DAE are defined.

2.5 Deriving the Differential Equations

The DAEs can not be used in a control problem, but rather to simulate the system on a computer. Therefore is it necessary to transform the DAEs into DEs that can be used for derivation of a controller.

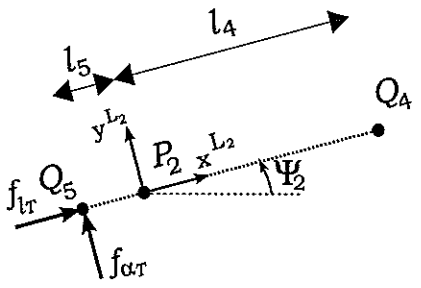

Figure 2.7: Definition of forces acting on trailer. f_l represents the longitudinal force and f_α represents the lateral force. Q_5 is the trailer wheel.

2.5.1 Global Symbolic Projection of DAE into DE

With the theory in [2] the DAE is mapped into the DE in a single step. The DAE is described in the form

$$\begin{aligned} \dot{\boldsymbol{p}} &= \boldsymbol{v} \\ M \cdot \dot{\boldsymbol{v}} &= \boldsymbol{f} + \boldsymbol{q}_G. \end{aligned} \tag{2.21}$$

To map the DAE to DE it's necessary to choose independent coordinates. There are 6 position variables and 2 constraint equations (2.20), therefore there are 2 dependent position variables and 4 independent. These can be chosen rather freely, but the following arguments are used.

The velocity of the car is important, therefore $x^R_{P_1O}$, $y^R_{P_1O}$ are chosen to be independent coordinates. Furthermore the car-trailer angle is important and according to figure 2.4 this means that ψ_1 and ψ_2 , which are used to calculate γ, should be independent coordinates. Therefore these 4 coordinates are chosen to be the independent coordinates.

Let the vector $\boldsymbol{p}_{\text{ind}}$ be the vector with the independent coordinates and let $\boldsymbol{p}_{\text{dep}}$ be the vector with the dependent coordinates. When the dependent and independent coordinates are chosen it is possible to define the projection matrices P_{rind} and P_{rdep} as

$$\begin{aligned} P_{\text{rind}} &= \frac{\partial \boldsymbol{p}_{\text{ind}}}{\partial \boldsymbol{p}} \\ P_{\text{rdep}} &= \frac{\partial \boldsymbol{p}_{\text{dep}}}{\partial \boldsymbol{p}}. \end{aligned} \tag{2.22}$$

With the constraints equations (2.20) it is possible to rewrite the dependent coordinates as

$$\boldsymbol{p}_{\text{dep}} = \begin{pmatrix} x^R_{P_2O} \\ y^R_{P_2O} \end{pmatrix} = \begin{pmatrix} x^R_{P_1O} - (l_3 + l_2) \cdot \cos\psi_1 - l_4 \cdot \cos\psi_2 \\ y^R_{P_1O} - (l_3 + l_2) \cdot \sin\psi_1 - l_4 \cdot \sin\psi_2 \end{pmatrix}. \tag{2.23}$$

Together with

$$\boldsymbol{p}_{\text{ind}} = \begin{pmatrix} x^R_{P_1O} \\ y^R_{P_1O} \\ \psi_1 \\ \psi_2 \end{pmatrix} \tag{2.24}$$

these equations yields the explicit constraints position equations

$$\boldsymbol{p} = \boldsymbol{h}(\boldsymbol{p}_{\text{ind}}) \tag{2.25}$$

that is shown in equation (A.15). Further is

$$\boldsymbol{h}_{\boldsymbol{p}_{\text{ind}}}(\boldsymbol{p}_{\text{ind}}) = \frac{\partial \boldsymbol{h}(\boldsymbol{p}_{\text{ind}})}{\partial \boldsymbol{p}_{\text{ind}}} \tag{2.26}$$

and is shown in equation (A.16). The spatial transform matrices are

$$T_{\text{ind}}(\boldsymbol{p}_{\text{ind}}) = I_4 \tag{2.27}$$

and

$$T = I_6 \tag{2.28}$$

due to a planar system. The global projector is defined as

$$J_v = T^{-1} \cdot h_{p_{\text{ind}}} \cdot T_{\text{ind}} = h_{p_{\text{ind}}} \tag{2.29}$$

and its time derivative is defined as

$$\dot{J}_v = \dot{h}_{p_{\text{ind}}}(p_{\text{ind}}). \tag{2.30}$$

$\dot{J}_v$ is shown in equation (A.20).

This provides the DE in the minimal coordinates p_{ind} and v_{ind}

$$\begin{aligned} \dot{p}_{\text{ind}} &= v_{\text{ind}} \\ M_{\text{ind}}(p_{\text{ind}}) \cdot \dot{v}_{\text{ind}} &= f_{\text{ind}}(p_{\text{ind}}, v_{\text{ind}}) + q_{G_{\text{ind}}}(p_{\text{ind}}, v_{\text{ind}}) \end{aligned} \tag{2.31}$$

where

$$M_{\text{ind}} = h_{p_{\text{ind}}}^T \cdot M \cdot h_{p_{\text{ind}}} \tag{2.32}$$

$$f_{\text{ind}} = h_{p_{\text{ind}}}^T \cdot f - h_{p_{\text{ind}}}^T \cdot M \cdot \dot{h}_{p_{\text{ind}}} \cdot v_{\text{ind}} \tag{2.33}$$

$$q_{G\text{ind}} = 0. \tag{2.34}$$

With this the goal is reached, the DEs are revealed. With help of the matrix inverse it is possible to rewrite the independent variables,

$$\dot{v}_{\text{ind}} = M_{\text{ind}}(p_{\text{ind}})^{-1} \cdot f_{\text{ind}}(p_{\text{ind}}, v_{\text{ind}}). \tag{2.35}$$

2.6 Force Estimation

The car and trailer moves as a result of forces acting on them. These forces are not measurable since they represent the friction force between the tire and the road. Therefore they must be estimated from known measurable variables. Force estimation in longitudinal direction can be estimated through the relation $F = m \cdot a$, where a is the acceleration of the car. Force estimation in the lateral direction requires more advanced theories about tire dynamics, see for example [3] and [4]. The estimated forces are used in the force matrix (2.10).

The velocity, acceleration and yaw rate for the mass center of the car are known from measurements in the car, through this it is possible to calculate the velocity, and the direction of the velocity, for other points on the car. In this case it is desirable to know the front and rear wheels velocity and direction of velocity.

2.6.1 Deriving Lateral Force

The lateral force has, according to [4], a linear relationship with the slip angle assuming small slip angles, see figure 2.8. That is

$$f_\alpha = -\alpha \cdot c_\alpha. \tag{2.36}$$

The constant c_α is known as the "cornering stiffness" and is said to depend on the properties of the tire, such as load and air pressure. In [5] there is the more detailed formula

$$c_\alpha = c_0 \cdot e^{\left(\frac{-c_0}{f_{\alpha_{max}}} \cdot |\alpha|\right)} \tag{2.37}$$

where $f_{\alpha_{max}}$ is the maximum available friction force in the lateral direction (read more about friction estimation in [6]).

More on Tire Cornering Stiffness, c_0

The c_0 is dependent of surface, temperature, weather and the load on the axle according to [4]. The load on the axle changes during driving because of wind resistance and acceleration. Therefore it is desirable to make c_0 a function of axle load. Let the forces be defined according to figure 2.9. The torque equations around the contact surface for each wheel and the torque equation around the towing hook are derived in the equations (A.27a) to (A.27d). From these equations the axle loads can be derived as in equation (A.28b) to (A.28d). With this it is possible to make c_0 dependent on the actual load on the wheel.

2.6.2 Calculation of Slip Angles

When there is angular velocity besides the normal velocity, the different points of the body move in different velocity compared to the velocity of the local frames origin. This is shown for the car in figure 2.10 and for the trailer in figure 2.11. Slip is defined as the difference in direction of velocity and heading direction of the tire, see figure 2.8. With known velocity and angular velocity it is possible to derive the velocity vector for the different points on the car and trailer.

Deriving Front Slip

The heading direction of the front wheel is not the same as the heading direction of the car because of the turning possibility. This means that it is necessary to subtract the turning angle from the angle between the velocity vector and the cars heading direction of the point Q_1 as seen in figure 2.12. The velocity vector

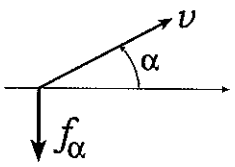

Figure 2.8: How the slip angle α creates lateral force f_α. The dotted line is the heading direction of the tire, v is the velocity vector and f_α is the induced force.

can be moved to the front with help of equations derived in [1]. It yields that

$$ {}^{R}\dot{r}^{R}_{PO} = {}^{R}\dot{r}^{R}_{P_1O} + A^{RL_1} \cdot \dot{r}^{L_1}_{PP_1} + \dot{\psi}_1 \cdot R \cdot \left(A^{RL_1} \cdot r^{L_1}_{PP_1} \right). \tag{2.38} $$

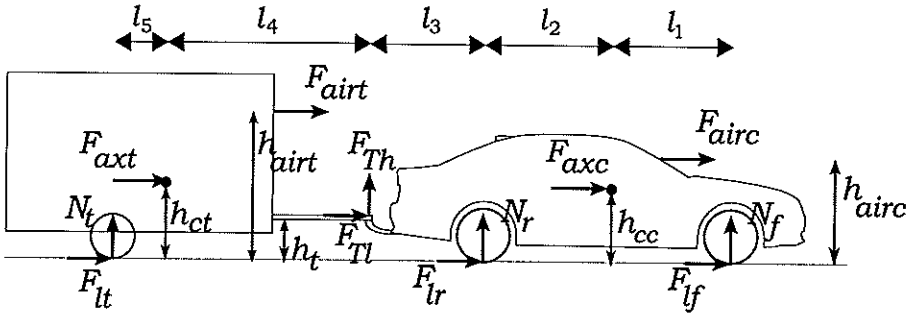

Figure 2.9: Definition of the longitudinal and horizontal forces acting on the car and the trailer. F_{airt} and F_{airc} is the force caused by air resistance. F_{axc} and F_{axt} is acceleration force acting on each body's mass center. F_{lt}, F_{lr} and F_{lf} are the longitudinal forces acting on the trailer wheel, the cars rear wheel and the cars front wheel. N_t, N_r and N_f are the horizontal forces acting between the trailer wheel, the cars rear wheel and the cars front wheel and the road. F_{Th} is the horizontal force acting between the trailer hook on the car and the trailer and F_{Tl} is the longitudinal force. h_{ct} and h_{cc} is the height of the mass center for the trailer respectively the car. h_{airt} and h_{airc} is the height where the force from air resistance is acting. h_t is the distance between the ground and the trailer hook.

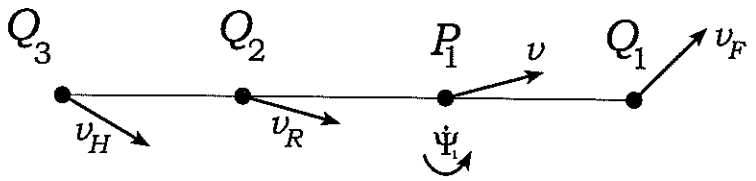

Figure 2.10: The different velocity vectors of the car.

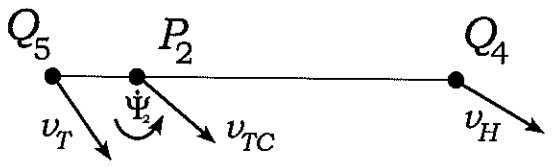

Figure 2.11: The different velocity vectors of the trailer.

This together with definitions according to figure 2.3 gives

$$\begin{aligned} r^R_{PP_1} &= r^R_{Q_1P_1} \\ \dot{r}^{L_1}_{Q_1P_1} &= 0 \\ r^{L_1}_{Q_1P_1} &= \begin{pmatrix} l_1 \\ 0 \end{pmatrix} \end{aligned} \tag{2.39}$$

and the equation can be rewritten as

$$v_F = v + \dot{\psi}_1 \cdot R \cdot \left(A^{RL_1} \cdot r^{L_1}_{Q_1P_1} \right). \tag{2.40}$$

The slip angle for the front wheel, α_F, is the angle between the front tires direction and v_F, see figure 2.12. This angle can be derived from

$$\alpha_F = \delta_F - \alpha \tag{2.41}$$

where α is derived from

$$\sin\alpha = \frac{v_F \times e^{L_1}_x}{|v_F| \cdot |e^{L_1}_x|} \tag{2.42}$$

yielding

$$\sin\alpha = \frac{-v_y \cdot \cos\psi_1 + v_x \cdot \sin\psi_1 - l_1 \cdot \dot{\psi}_1}{\sqrt{|v|^2 + 2l_1 \cdot \dot{\psi}_1 \left(v_y \cdot \cos\psi_1 - v_x \cdot \sin\psi_1\right) + l_2^2\dot{\psi}_1^2}}. \tag{2.43}$$

Deriving Rear slip

With help of equation (2.38) derivation of the rear slip is straight forward. This time

$$\begin{aligned} r^R_{PP_1} &= r^R_{Q_2P_1} \\ r^{L_1}_{Q_2P_1} &= \begin{pmatrix} -l_2 \\ 0 \end{pmatrix} \end{aligned} \tag{2.44}$$

giving

$$v_R = v + \dot{\psi}_1 \cdot R \cdot \left(A^{RL_1} \cdot r^{L_1}_{Q_2P_1} \right). \tag{2.45}$$

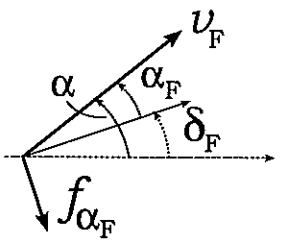

Figure 2.12: The slip angle α_F for the front wheel.

The rear slip angle, α_R, can now be derived according to (2.42)

$$\sin\alpha_R = \frac{-v_y \cdot \cos\psi_1 + v_x \cdot \sin\psi_1 + l_2 \cdot \dot{\psi}_1}{\sqrt{|v|^2 + 2l_2 \cdot \dot{\psi}_1 \left(v_x \cdot \sin\psi_1 - v_y \cdot \cos\psi_1\right) + l_2^2\dot{\psi}_1^2}}. \tag{2.46}$$

Deriving Trailer Slip

By transforming the velocity vector to the trailer wheel it is possible to estimate the trailer's slip. This is done according to earlier derivations. With help from equation (2.38) it yields

$$ {}^R\dot{\boldsymbol{r}}^R_{Q_3O} = {}^R\dot{\boldsymbol{r}}^R_{P_1O} + \dot{\psi}_1 \cdot R \cdot \left(A^{RL_1} \cdot \boldsymbol{r}^{L_1}_{Q_3P_1}\right) \tag{2.47}$$

$$ {}^R\dot{\boldsymbol{r}}^R_{Q_4O} = {}^R\dot{\boldsymbol{r}}^R_{P_2O} + \dot{\psi}_2 \cdot R \cdot \left(A^{RL_2} \cdot \boldsymbol{r}^{L_2}_{Q_4P_2}\right) \tag{2.48}$$

$$ {}^R\dot{\boldsymbol{r}}^R_{Q_5O} = {}^R\dot{\boldsymbol{r}}^R_{P_2O} + \dot{\psi}_2 \cdot R \cdot \left(A^{RL_2} \cdot \boldsymbol{r}^{L_2}_{Q_5P_2}\right). \tag{2.49}$$

Here ${}^R\dot{\boldsymbol{r}}^R_{Q_5O}$ is the searched variable. Adding one of the existing constraints

$$ {}^R\dot{\boldsymbol{r}}^R_{Q_3O} = {}^R\dot{\boldsymbol{r}}^R_{Q_4O} \tag{2.50}$$

makes it possible to derive ${}^R\dot{\boldsymbol{r}}^R_{P_2O}$ as

$$ {}^R\dot{\boldsymbol{r}}^R_{P_2O} = {}^R\dot{\boldsymbol{r}}^R_{P_1O} + \dot{\psi}_1 \cdot R \cdot \left(A^{RL_1} \cdot \boldsymbol{r}^{L_1}_{Q_3P_1}\right) - \dot{\psi}_2 \cdot R \cdot \left(A^{RL_2} \cdot \boldsymbol{r}^{L_2}_{Q_4P_2}\right). \tag{2.51}$$

This yields that

$$\begin{aligned} {}^R\dot{\boldsymbol{r}}^R_{Q_5O} = {}& {}^R\dot{\boldsymbol{r}}^R_{P_1O} + \dot{\psi}_1 \cdot R \cdot \left(A^{RL_1} \cdot \boldsymbol{r}^{L_1}_{Q_3P_1}\right) \\ & - \dot{\psi}_2 \cdot R \cdot \left(A^{RL_2} \cdot \boldsymbol{r}^{L_2}_{Q_4P_2}\right) \\ & + \dot{\psi}_2 \cdot R \cdot \left(A^{RL_2} \cdot \boldsymbol{r}^{L_2}_{Q_5P_2}\right) \\ = {}& {}^R\dot{\boldsymbol{r}}^R_{P_1O} + \dot{\psi}_1 \cdot R \cdot \left(A^{RL_1} \cdot \boldsymbol{r}^{L_1}_{Q_3P_1}\right) \\ & + \dot{\psi}_2 \cdot R \cdot \left(A^{RL_2} \cdot \left(\boldsymbol{r}^{L_2}_{Q_5P_2} - \boldsymbol{r}^{L_2}_{Q_4P_2}\right)\right) \end{aligned} \tag{2.52}$$

which together with

$$\sin\alpha_T = \frac{v_T \times e_x^{L_2}}{|v_T| \cdot |e_x^{L_2}|} \tag{2.53}$$

gives

$$\sin\alpha_T = \frac{v_y \cdot \cos\psi_2 - v_x \cdot \sin\psi_2 - (l_4 + l_5) \cdot \dot{\psi}_2 - (l_2 + l_3) \cdot \cos(\psi_1 - \psi_2) \cdot \dot{\psi}_1}{\sqrt{\begin{array}{l} |v|^2 + (l_2 + l_3)^2 \cdot \dot{\psi}_1^2 + (l_4 + l_5)^2 \cdot \dot{\psi}_2^2 \\ \quad +2(l_2 + l_3)(v_x \cdot \sin\psi_1 - v_y \cdot \cos\psi_1) \cdot \dot{\psi}_1 \\ \quad +2(l_4 + l_5)(v_x \cdot \sin\psi_2 - v_y \cdot \cos\psi_2) \cdot \dot{\psi}_2 \\ \quad +2(l_2 + l_3) \cdot (l_4 + l_5) \cdot \cos(\psi_1 - \psi_2) \cdot \dot{\psi}_1 \cdot \dot{\psi}_2 \end{array}}} \tag{2.54}$$

Possible Problems with Slip Estimation

The velocity of the vehicle must be unequal zero. At zero is it not possible to calculate the slip since the denominator in the equations (2.42), (2.46) and (2.54) turns zero. It is obvious that when the car is not moving, there is no slip.

Observe that the slip estimations are estimations of the model's slip, not the real system's slip. Under the circumstances that the model and its parameters are accurate the slip of the model will be the same as the slip of the real system.

2.6.3 Longitudinal Force Estimations

It is possible to achieve a longitudinal force estimation with help of brake pressure, engine torque and a correction factor from the difference between the models velocity and the real systems velocity.

Rear Wheel

Since the car has rear wheel traction, it is a good approximation that engine torque after the transmission losses transforms to longitudinal force in the rear wheels. When the car is braking the approximation that the deceleration force is split equally between front and rear wheels is used. The normal split when the car is driving without the trailer is 70/30 between front/rear wheels, but here the assumption that the trailer weight shifts the split toward the rear wheels is made.

Front Wheel

For the front wheels all longitudinal force originates from braking force. The braking force is as stated earlier split equally between front and rear wheels and calculated from deceleration.

Trailer Wheel

The trailer brake actuator is connected to the towing hook. During braking the trailer is pressed toward the car and a spring, connected to the trailer brake, gets pressed together and the trailer starts to brake. Therefore the assumption is made that braking force is proportional to the deceleration, but only when the car brakes.

2.7 Finalize the Model

2.7.1 Optimizing Variables

When the model is simulated the first time, all of the constants are calculated approximations or taken from either [5] or [6]. To make the model accurate these variables are optimized using a nonlinear optimization algorithm.

2.7.2 Model Validation

The model is validated with input data from test drives. The results seen in figure 2.14 to figure 2.18 shows that the model is fairly accurate.

A sketch of the test track where the test drives were performed is shown in figure 2.13. The dotted line displays the car's trajectory.

In figure 2.14 are the position coordinates calculated during a test drive drawn. There exists a drift between each lap, but this is small enough to make the statement that the model is accurate. This can be compared with the position coordinates calculated according to the kinematic model in [7] and is displayed in figure 2.15. It is clear that the drift of the model stated here is less then the drift in the kinematic model.

Figure 2.16 is a plot of the car-trailer angle, γ, during a test drive. The speed during the test drive was around 50 km/h, somewhat slower around the corners. It is clear that the modeled car-trailer angle matches the measured angle very well. Figure 2.17 displays a magnification of figure 2.16. It also contains the car-trailer angle modeled by the kinematic model stated in [7].

Figure 2.18 is a plot of the car's yaw rate, $\dot{\psi}_1$, during the same test drive as in figure 2.16. Here is it clear that the modeled car yaw rate is accurate. Figure 2.19 displays a magnification of figure 2.18. It also contains the car yaw rate modeled by the kinematic model stated in [7].

A way to describe the difference between the different models and the actual system is to calculate the root mean square error

$$RMSE = \sqrt{\frac{1}{n}\sum (x_{meas} - x_{calc})^2} \tag{2.55}$$

where n is the number of samples, x_{meas} is the measured variable value and x_{calc} is the modeled variable value. This makes it possible to compare the two models as seen in table 2.1. The $RMSE$ values shows that for the yaw rate the

Table 2.1: The $RMSE$ values of the different models and the different states.

Model	$RMSE$ for the yaw rate	$RMSE$ for the car-trailer angle
Kinetic model stated here	0.008	0.017
Kinematic model stated in [7]	0.040	0.037

kinetic model is twice as good as the kinematic model, but only slightly worse for the car-trailer angle.

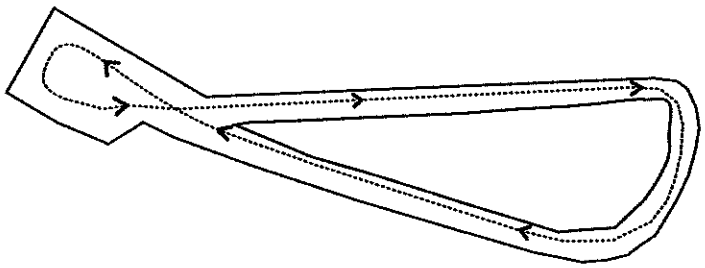

Figure 2.13: Simple sketch of the ZFLS test track. The dotted line indicates the driving trajectory during test drives.

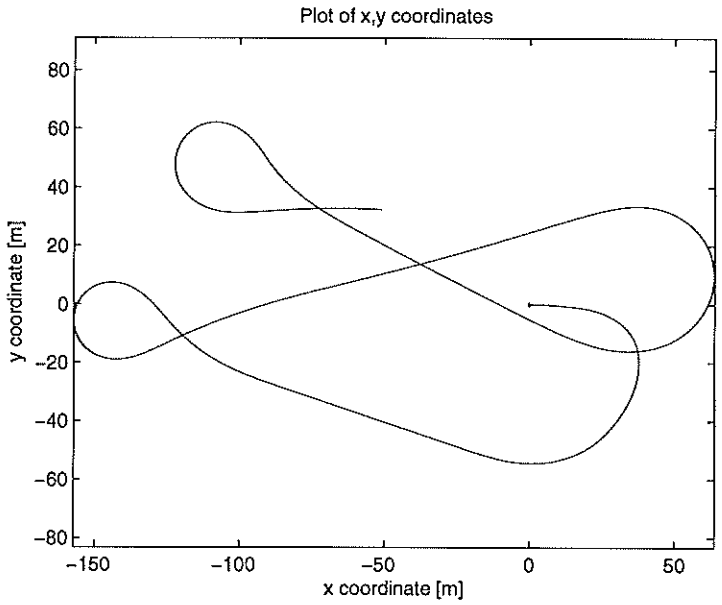

Figure 2.14: After a simulation the following x,y coordinates were calculated. The simulation input data is taken during driving around the test track with speeds around 50 km/h, somewhat slower in the turns. Even though all movements of the car and trailer comes from estimated forces that are calculated with help of estimated slip angles, the coordinates represent the driving trajectory well. After one lap it differs about 30 meters in y-direction and 35 meters in x-direction which shows how well the approximations works. The red dot in the origin shows the start point.

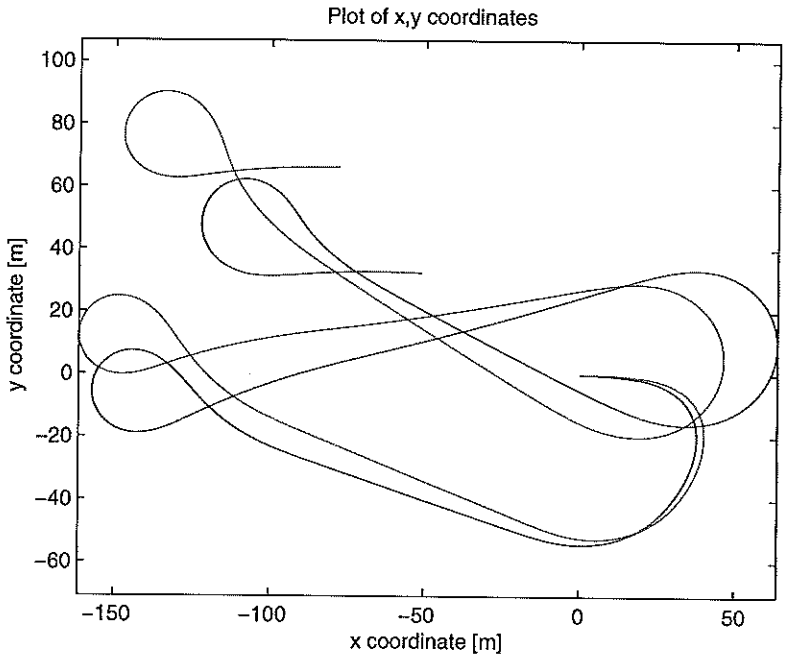

Figure 2.15: Comparison of the kinetic model derived here (blue line) and the kinematic model derived in [7] (red line). Same test drive as in figure 2.14.

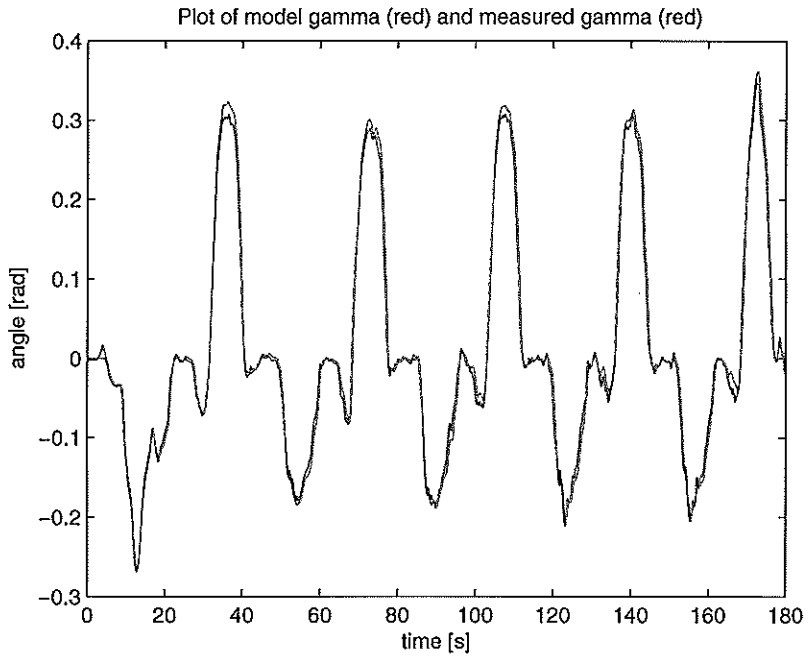

Figure 2.16: Comparison of the calculated gamma (red) and the measured (blue). Data collected during test drive in speeds around 50 km/h. Positive angle indicates left turn, and is performed in the small circle on the test track, see figure 2.14.

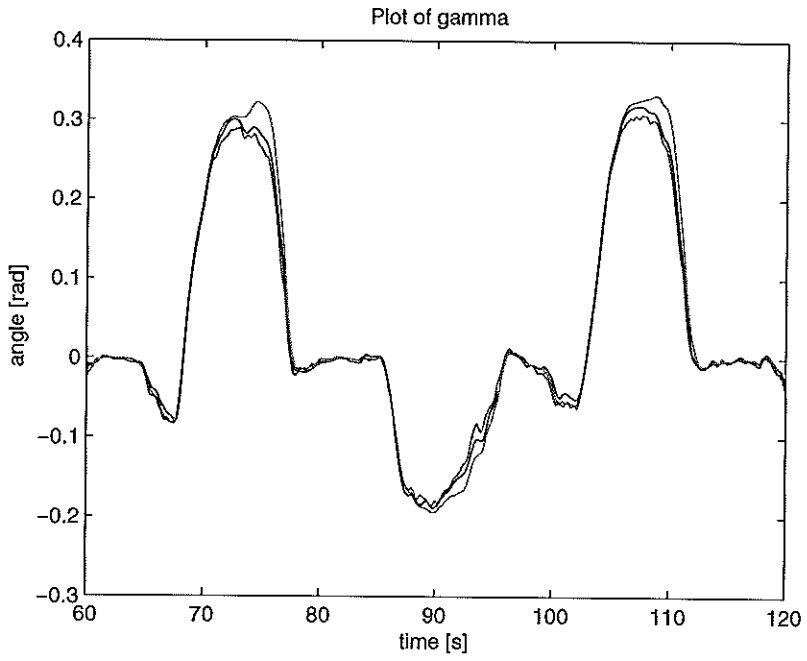

Figure 2.17: Comparison of the calculated model γ (blue), γ from the kinematic model in [7] (red) and the measured γ (black). This is a magnified graph of figure 2.16. The graph indicates that this model is better then the kinematic model during hard cornering.

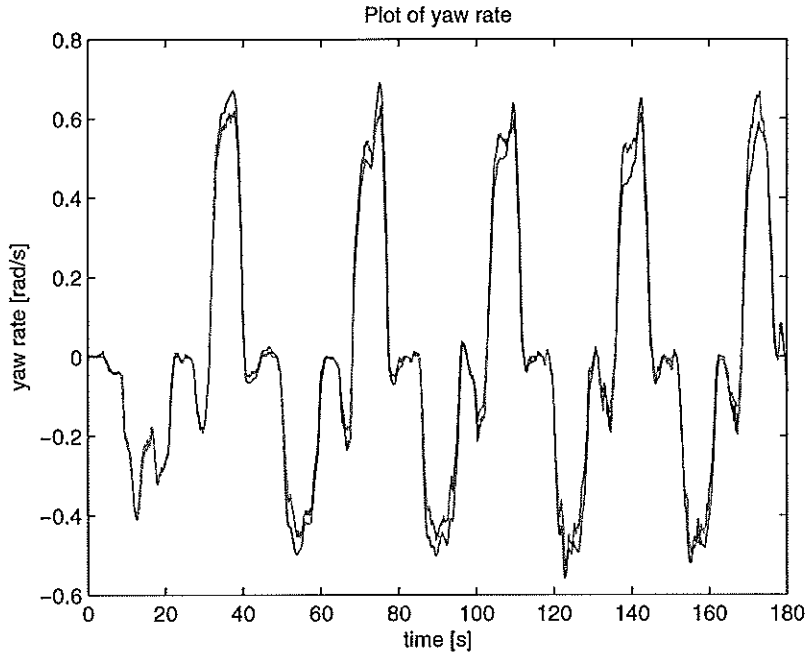

Figure 2.18: Comparison of the calculated yaw rate of the model (red) and the measured (blue). Data collected during the same test drive as in figure 2.16. Positive value of the yaw rate indicates left turn, and is performed in the small circle on the test track, see figure 2.14.

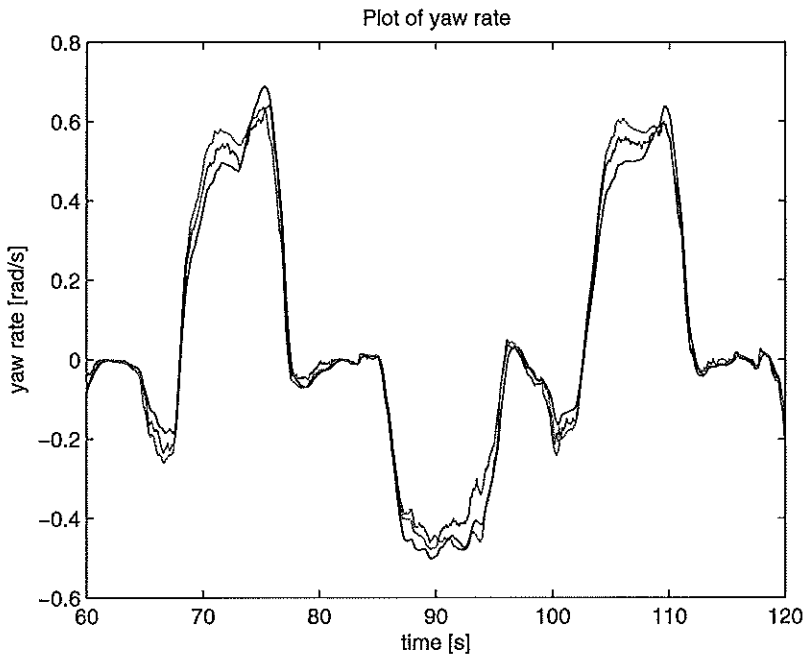

Figure 2.19: Comparison of the calculated yaw rate of the model (blue), the model derived in [7] (red) and the measured (black). This is a magnified graph of figure 2.18.

Chapter 3

Derivation of Controllers

In this chapter two different controllers are derived for three of the system states. The controllers derived are a linear controller for a linearized version of the model and a feedback linearization controller. The three system states that are controlled are the yaw rate of the car, the car-trailer angle and the time derivative of the car-trailer angle. The control signal is the front wheel angle, δ_F, since this is what the AFS-system can control.

3.1 Controlling Nonlinear Systems

One way to control a nonlinear system is to linearize the system around a working point, and then calculate control parameters for the linearized system. More advanced theory about controlling nonlinear systems can be found in [8]. The linearization feedback method from [8] is used in this thesis.

3.2 States to Control

The system is built up by 8 DEs, the following state space variables and control signals are defined.

$$\begin{aligned} u &= \delta_F \\ \begin{cases} x_1 &= x^R_{P_1O} \\ x_2 &= v^R_{x_1} \\ x_3 &= y^R_{P_1O} \\ x_4 &= v^R_{y_1} \\ x_5 &= \psi_1 \\ x_6 &= \dot{\psi}_1 \\ x_7 &= \psi_2 \\ x_8 &= \dot{\psi}_2 \end{cases} \end{aligned} \tag{3.1}$$

Three of these or combination of these may be of interest: $\dot{\psi}_1$, $\gamma = \psi_1 - \psi_2$ and $\dot{\gamma} = \dot{\psi}_1 - \dot{\psi}_2$, that is the car yaw rate, the car-trailer angle and the car-trailer

angle derivative respectively.

3.3 Controller for the Linearized Model

A way to reach a linear system to control, is to linearize the nonlinear system around a working point. The nonlinear system

$$\dot{x} = f(x, z, u) \tag{3.2}$$

is linearized around a working point (x_0, u_0).

$$\dot{z} = Az + Bv \tag{3.3}$$

where

$$\begin{aligned} z &= x - x_0 \\ v &= u - u_0 \\ A &= \begin{pmatrix} \frac{\partial f_1}{\partial x_1} & \cdots & \frac{\partial f_1}{\partial x_8} \\ \vdots & \ddots & \vdots \\ \frac{\partial f_8}{\partial x_1} & \cdots & \frac{\partial f_8}{\partial x_8} \end{pmatrix}_{(x_0,u_0)} \\ B &= \begin{pmatrix} \frac{\partial f_1}{\partial u} \\ \vdots \\ \frac{\partial f_8}{\partial u} \end{pmatrix}_{(x_0,u_0)} . \end{aligned} \tag{3.4}$$

Here A and B is said to be the Jacobian matrices of f with respect to x and u respectively evaluated at the point (x_0, u_0). When the A and B matrices are calculated, it is possible to make an attempt to derive a controller that stabilizes the system.

3.4 Feedback Linearization

According to [8] feedback linearization is a way to linearize the nonlinear system, making it possible to apply well known linear controlling. If a system is described as

$$x^{(n)} = f(x) + g(x) \cdot u \tag{3.5}$$

and has no zeros in the right half-plane it is possible to apply feedback linearization. In this case for the car with trailer there are four equations like this

$$\dot{x}_{2i} = f_i(x, z, u) + g_i(x, z, u) \cdot u \qquad i = 1, 2, 3, 4 \tag{3.6}$$

and four equations like

$$\dot{x}_{2i-1} = x_{2i} \qquad i = 1, 2, 3, 4 \tag{3.7}$$

and depending on what variable to control, we define the system outputs

$$\begin{aligned} y_1 &= x_6 && (\dot{\psi}_1) \\ y_2 &= x_5 - x_7 && (\gamma) \\ y_3 &= x_6 - x_8 && (\dot{\gamma}) \end{aligned} \tag{3.8}$$

3.4.1 Yaw Rate Controller

Controlling the yaw rate means controlling y_1 in equation (3.8). The system looks like

$$\begin{aligned} \dot{x}_6 &= f_3(x,z,u) + g_3(x,z,u) \cdot u \\ y &= x_6. \end{aligned} \tag{3.9}$$

Since there is no direct relationship between y and u we differentiate y one time, giving

$$\dot{y} = \dot{x}_6 \tag{3.10a}$$

$$= f_3(x,z,u) + g_3(x,z,u) \cdot u. \tag{3.10b}$$

The feedback linearization is introduced by introducing the new variable w that is chosen in the way

$$u = \frac{1}{g_3(x,z,u)}(w - f_3(x,z,u)). \tag{3.11}$$

Inserting this u in equation (3.10b) gives

$$\begin{aligned} \dot{y} &= f_3(x,z,u) + g_3(x,z,u) \cdot \frac{1}{g_3(x,z,u)}(w - f_3(x,z,u)) \\ &= f_3(x,z,u) + (w - f_3(x,z,u)) \\ &= w. \end{aligned} \tag{3.12}$$

This supplies a simple integrator relationship between the yaw rate and the new input

$$\dot{y} = w \tag{3.13}$$

which simplifies the controlling into controlling a linear system.

Desired Yaw Rate

The normal input to the system is the steering wheel angle, but that signal does not contain any information about how the driver desires the car to behave. Therefore it is necessary to find out the yaw rate the driver expects for a given steering wheel angle and a given velocity. By comparing the desired yaw rate and the actual yaw rate it is then possible to adjust the front wheel angle so that the actual yaw rate changes toward the desired yaw rate.

According to [3] the yaw rate at steady state driving can be calculated as

$$\begin{aligned}\dot{\psi} &= \delta_F \frac{v_x}{(l_1+l_2)+\frac{K_{us}v_x^2}{g}} \\ &= \frac{\delta_F}{l_1+l_2}\cdot\frac{v_x}{1+\frac{K_{us}}{(l_1+l_2)g}v_x^2} \\ &= \frac{\delta_F}{l_1+l_2}\cdot\frac{v_x}{1+\left(\frac{v_x}{v_{car}}\right)^2}, \\ \text{if} \quad v_{car}^2 &= \frac{(l_1+l_2)g}{K_{us}}.\end{aligned} \tag{3.14}$$

Here v_{car} is the characteristic velocity of the car, the velocity where the highest yaw rate gain, $\dot{\psi}_1/\delta_F$, is achieved. This parameter can be measured from test drives.

Using this equation to calculate the desired yaw rate is not entirely correct, since the driver might expect a slightly different behavior when driving with the trailer. Still the behavior can be expected not to differ too much, and therefore this equation is used.

PD-Controller

The system can be controlled with a PD-controller which calculates the linear controll signal w. The choice of linear controller is based on tests with different controllers during test drives. In [9] the discrete derivative of the controller is derived as

$$D(kh) = \frac{T_d}{T_d+Nh}D(kh-h) - \frac{KT_dN}{T_d+Nh}\left(y_{ref}(kh)-y_{ref}(kh-h)\right) \tag{3.15}$$

which has a high pass filter (N) implemented, and h is the sample time.

3.4.2 γ Controller

Controlling γ means controlling y_2 in equation (3.8). This concerns the system

$$\begin{aligned}\dot{x}_5 &= x_6 \\ \dot{x}_6 &= f_3(x,z,u)+g_3(x,z,u)\cdot u \\ \dot{x}_7 &= x_8 \\ \dot{x}_8 &= f_4(x,z,u)+g_4(x,z,u)\cdot u \\ y &= x_5 - x_7\end{aligned} \tag{3.16}$$

Since there is no direct relationship between y and u we differentiate y until there is a direct relationship between y and u, giving

$$\begin{aligned}
\dot{y} &= \dot{x}_5 - \dot{x}_7 \\
&= x_6 - x_8 \\
\ddot{y} &= \dot{x}_6 - \dot{x}_8 \\
&= (f_3(x,z,u) + g_3(x,z,u)\cdot u) \\
&\quad - (f_4(x,z,u) + g_4(x,z,u)\cdot u) \\
&= (f_3(x,z,u) - f_4(x,z,u)) \\
&\quad (g_3(x,z,u) - g_4(x,z,u))\cdot u.
\end{aligned} \tag{3.17}$$

With this information it is now possible to apply the earlier stated theory.

Desired γ

In [7] it is showed that for each front wheel angle δ_F there exists one unique car-trailer angle, γ, where the system is in equilibrium. For a front wheel angle δ_F the equilibrium car-trailer angle γ is

$$\gamma = \arcsin\left(\frac{(l_4+l_5)\tan\delta_F}{\sqrt{(l_1+l_2)^2 + l_3^2\tan^2\delta_F}}\right) + \arctan\left(\frac{l_3\tan\delta_F}{l_1+l_2}\right). \tag{3.18}$$

PID controller

The linearization feedback system was controlled with a PID controller, with anti windup implemented. The choice of linear controller is based on tests with different controllers during test drives.

3.4.3 $\dot{\gamma}$ Controller

Controlling $\dot{\gamma}$ means controlling y_3 in equation (3.8). This concerns the system

$$\begin{aligned}
\dot{x}_6 &= f_3(x,z,u) + g_3(x,z,u)\cdot u \\
\dot{x}_8 &= f_4(x,z,u) + g_4(x,z,u)\cdot u \\
y &= x_6 - x_8
\end{aligned} \tag{3.19}$$

and since there is no direct relationship between y and u we differentiate y until there is a direct relationship between y and u, giving

$$\begin{aligned}
\dot{y} &= \dot{x}_6 - \dot{x}_8 \\
&= (f_3(x,z,u) + g_3(x,z,u)\cdot u) \\
&\quad - (f_4(x,z,u) + g_4(x,z,u)\cdot u) \\
&= (f_3(x,z,u) - f_4(x,z,u)) \\
&\quad (g_3(x,z,u) - g_4(x,z,u))\cdot u.
\end{aligned} \tag{3.20}$$

Desired $\dot{\gamma}$

Under the assumption that no lateral slip exists, the differential equation for the car-trailer angle can be derived as in [7], giving

$$\dot{\gamma} = v\left(\frac{1}{l_1+l_2} + \frac{l_3}{(l_1+l_2)(l_4+l_5)}\cos\gamma\right)\tan\delta_F - \frac{v}{l_4+l_5}\sin\gamma \qquad (3.21)$$

which is used as a reference value for $\dot{\gamma}$. Observe that in the implementation γ is the measured value, and not the model value. v is the measured speed of the car.

PID controller

The linearization feedback system was controlled with a PID controller, with anti windup implemented. The choice of linear controller is based on tests with different controllers during test drives.

3.5 A First Evaluation of the Controllers

Test drives were made to find out how the different controllers could follow their reference value. These are test drives with speeds around 15-20 km/h, without any instability. During these test drives the steering wheel is only used as a reference value to the controller, and the controller uses the AFS-system to apply a front wheel angle. Thus might it feel strange to maneuver the car since the front wheel angle may not behave as usual.

A controller is said to work, if it feels like driving the car as if there were no controller.

3.5.1 Yaw Rate Controller

Linearization Feedback

This controller worked good. Except for a delay between the reference signal and the measured signal, this was like driving the car normally.

Linearized Controller

Here was the reference following terrible. Almost impossible to drive the car because a large delay between the reference value and the measured signal.

3.5.2 γ Controller

Neither the linearization feedback or the linearized controller works. There was a large delay between the reference value and the measured value. This is probably because how the reference value is calculated.

3.5.3 $\dot{\gamma}$ Controller

Here is the same problem as with the γ controller and also here it is probably because the reference value calculation is not suitable for this application.

3.5.4 Conclusion

Since only the linearization feedback controller for the yaw rate works only this will be further investigated.

3.6 Robustness and Stability Analysis

It is to be shown that if the feedback linearization is exact, the system will be stabilized by a normal simple proportional controller. Further it is to be investigated how the feedback linearization will function when the system differs from the model.

3.6.1 Difference Between Model and System

As the model is not exact, the linearization feedback will not linearize the system as desired. With the assumption that it will remove nonlinearities, but not perfect, the remaining nonlinearity can be seen as a noise on the system input, v. If the system with linearization feedback is linearized around a working point, the system can be investigated to see how the system looks from v to y.

With exact feedback linearization the new control signal u will be derived as

$$u = (w - f)\frac{1}{g}. \tag{3.22}$$

If there exists an error in the f and g, the feedback linearization can be derived as

$$\begin{aligned} u &= (w - (f + \Delta f))\left(\frac{1}{g} + \Delta g\right) \\ &= (w - f)\frac{1}{g} + \left(w\Delta g - f\Delta g - \frac{\Delta f}{g} - \Delta f \Delta g\right) \end{aligned} \tag{3.23}$$

If there is a disturbance v on the input to the feedback linearization the output can be written as

$$u = (v + w - f)\frac{1}{g} = \frac{v}{g} + \frac{w}{g} - \frac{f}{g}. \tag{3.24}$$

It is desired that the error in the feedback linearization is modeled as noise on the input, therefore there is an equality between (3.23) and (3.24) that can

be written as

$$\begin{aligned}
\frac{v}{g}+\frac{w-f}{g} &= \frac{w-f}{g}+\left(w\Delta g - f\Delta g - \frac{\Delta f}{g} - \Delta f\Delta g\right) \Rightarrow \\
\frac{v}{g} &= \left(w\Delta g - f\Delta g - \frac{\Delta f}{g} - \Delta f\Delta g\right) \Rightarrow \\
v &= \left(w\Delta g - f\Delta g - \frac{\Delta f}{g} - \Delta f\Delta g\right)\cdot g \\
&= w\cdot g\cdot \Delta g - f\cdot g\cdot \Delta g - \Delta f - g\cdot \Delta f\cdot \Delta g \\
&= (w-(f+\Delta f))\cdot g\cdot \Delta g - \Delta f.
\end{aligned} \tag{3.25}$$

This means that the error in the feedback linearization due to an inaccurate model can be modeled as noise according to (3.25). For the noise to be small, the following is stated

$$v \to 0 \quad \text{if} \quad \Delta g \to 0, \Delta f \to 0 \tag{3.26}$$

which is the case when there is no error in the feedback linearization.

It is worth mentioning is that an error in f gives an offset error when only using a proportional controller, and an error in g gives the wrong dynamic of the controller, and an offset error. g can be seen as a modifier of the controller's proportional gain.

By examine the the transfer function from v to y, see figure 3.1, it is clear that the noise will be suppressed. The system is said to be stable if the error in the feedback linearization is bounded,

$$|v| \leq v_{max}. \tag{3.27}$$

Although it is theoretical possible to use a very large gain in the proportional controller, this would lead to a nondesired behavior of the control signal, mainly because of the interaction of the actuator and the steering wheel. It is desired that the vehicle has the same behavior with the controller as without in safe situations.

3.6.2 Simulating Stability Limits

Because of the lack of good theory on robustness and stability of the linearization feedback the system was simulated in order to find stability borders for the different parameters. The simulations were performed with two simulated car-trailer models, where one was acting as the real system on which the parameters were changed. Only the parameters concerning the trailer were changed, as the car parameters are said to be known. One parameter at a time was changed, if nothing else is stated.

The system was simulated to turn for a few seconds, and then drive straight again. If the controller managed to stabilize the car-trailer after and during the turn, the system was said to be stable.

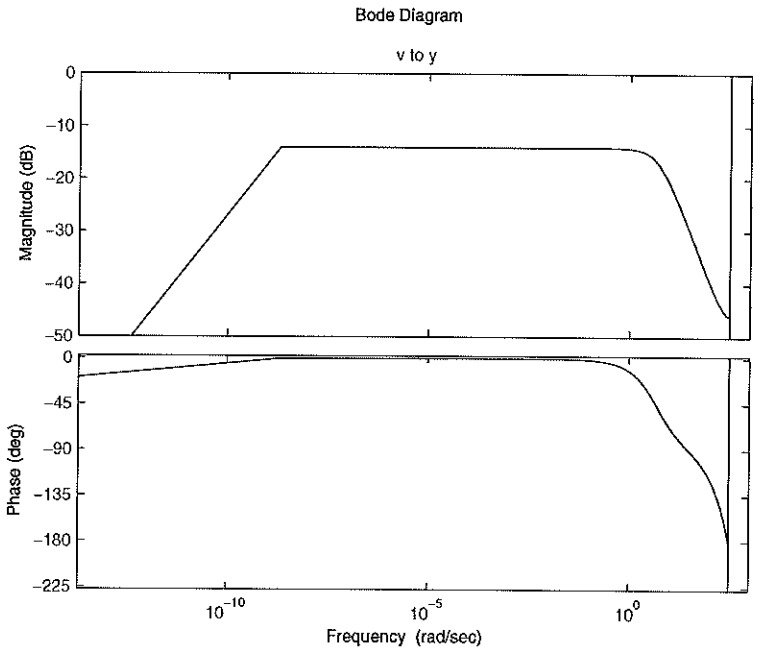

Figure 3.1: Bode diagram over the transfer function from v to y.

Results

The simulations showed how much it was possible to change the parameter value compared to its nominal value. The permitted changes are shown in table 3.1, figure 3.2 and figure 3.3.

Table 3.1: The range of possible change of different parameters with maintained stability of the controller.

Parameter	Range of change
c_3	60% – 1000%
m_2	0% – 146%
J_2	0% – 154%

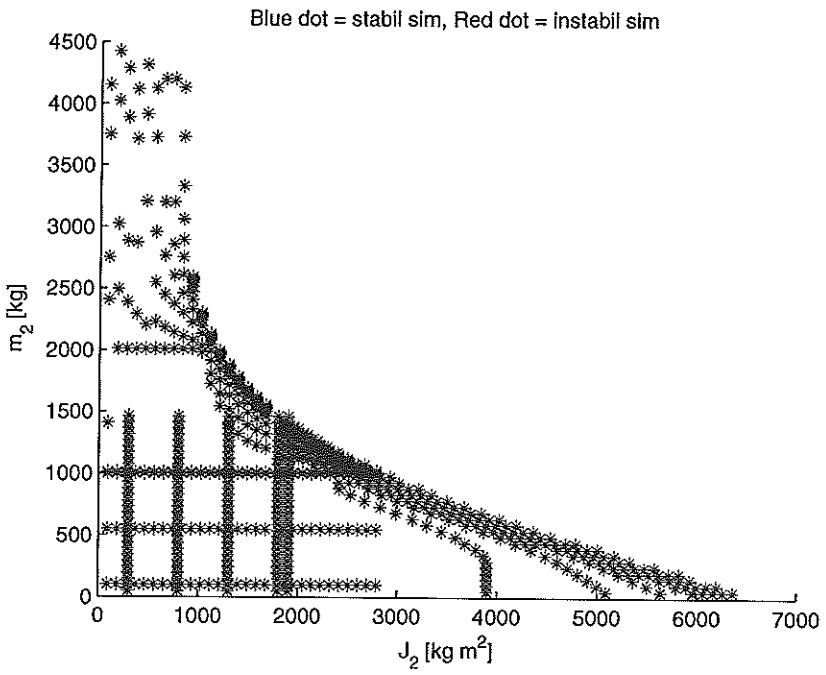

Figure 3.2: Area of stability when changing the mass of the trailer and the moment of inertia at the same time. A blue dot represents a stable simulation, a red dot represents an unstable simulation.

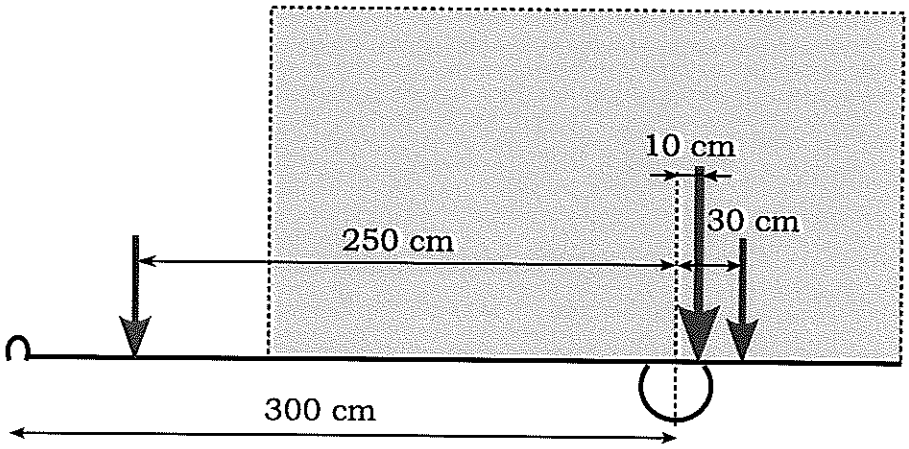

Figure 3.3: Area of stability when changing load placement on the trailer, l_5. The red arrow shows the nominal value, and the blue arrows how far from the red arrow it is possible to move the mass center.

Chapter 4

Implementation and Evaluation of the Controller

In this chapter is the controller implemented and evaluated.

4.1 Implementing Feedback Linearization

The feedback linearization is theoretical a perfect way of making a nonlinear system linear. But it demands a very good model and even better knowledge of the parameters in the model. The model stated here is good, but not perfect which might lead to the worse performance of the controller.

In this situation there is a feedback from the actuator to the device creating the reference value, the steering wheel. This means that when the actuator makes fast movements, this will move the reference value and possibly inducing unwanted oscillations. To avoid this it is necessary that the control signal is bounded, which is achieved by using a low proportional gain. This means worse performance which is avoided by using a feed forward from the reference signal to the controller signal.

4.1.1 Controlling Area Constrains

The controller is not supposed to be acting at all time, only at high velocity driving without too much cornering. This is solved by a variable maximal AFS motor angle. This is done with a lookup table that uses speed as input and the maximal AFS motor angle as output, at low speeds (<30 km/h) the maximal AFS motor angle is 0°.

4.1.2 Tuning the Controller to get the right Driving Feeling

The setup with a bounded AFS motor angle turned out to be rather good, but it still did not feel like driving a car. Likewise it is not desirable that the controller

acts when the driver controls the car with trailer well enough, compared to how the controller would do. The solution is to introduce a dead zone for the AFS motor angle, meaning that the motor will only interact when the difference between the controller desired δ_F and of the driver applied δ_F. How dead zone works together with a saturation of the output signal is shown in figure 4.1.

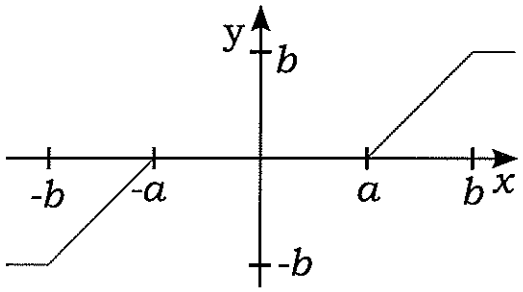

Figure 4.1: The function of a dead zone together with a saturation. When the input magnitude ($|x|$) is below a certain level a, the output (y) is zero. When the input magnitude is between a and b, the output will be $(x-a)$ or $(a-x)$ depending on the sign of x. When $|x-a|$ is greater then b, the output will be b or $-b$ depending on the sign of x.

By driving tests it is shown that the decision where to intervene is speed dependent. At normal speeds (70 km/h) a dead zone of 2.5° on the front wheel angle, δ_F, will prevent unnecessary interaction, and still help the driver in critical situations. For safety reasons the AFS motor is prevented to add more then 5° on the front wheel angle, which in most situations is less then what the controller ever puts as desired value.

Since a certain error is accepted it is not possible to have any integral part in the controller.

4.1.3 Snake Behavior of the Trailer

One special case when the dead zone should be minimized is when the trailer starts to snake. This very dangerous behavior can make the trailer tip over, or in worst case make the trailer go all the way around and hit the car in the side.

What is Snake Behavior?

When the trailer starts to go from side to side behind the car, even if the car is driving straight, it is called snake behavior of the trailer. This dangerous oscillation often starts after hitting a small hole or a small bump in the road or because of side wind, and is very hard, if not impossible, to maneuver away. Most often the oscillation decreases in amplitude when one keeps on driving steady, but with a badly loaded trailer and high speed the oscillations might increase.

Another way to induce the oscillation is to make a fast lane change. It seems that the oscillation is a result of the moment of inertia. First the yaw rate of the car increased and then decreased again, like a sinus curve. When the car drives straight again, the lateral forces that are needed to keep the trailer straight are too small.

Detecting the Snake Behavior

When the trailer moves from side to side behind the car it causes the car to move from side to side. These movements can be seen on the yaw rate sensor, and be compared to the desired yaw rate. When driving straight with snake behavior the desired yaw rate is constant, while the measured value has a sinus form. This implies that the controller should be able to stabilize the car if the dead zone is small enough.

Examine the desired γ and the measured γ shows the same relationship, the desired value is constant, while the measured has a sinus form. For the measured γ the oscillation is much clearer and can be discovered earlier compared to the measured yaw rate, see figure 4.5. Therefore the error between the desired γ and the measured γ is used for the snake detection.

The error between the measured γ and the desired γ is put through a high pass filter, and then a dead zone with offset is applied. Integrating the modified signal when it reaches above a certain level lim, and using a negative feedback to the integrator when the modified signal is below lim, the integrated signal is said to be a measurement of how much the trailer is oscillating. A block diagram of the snake detection can be seen in figure 4.2

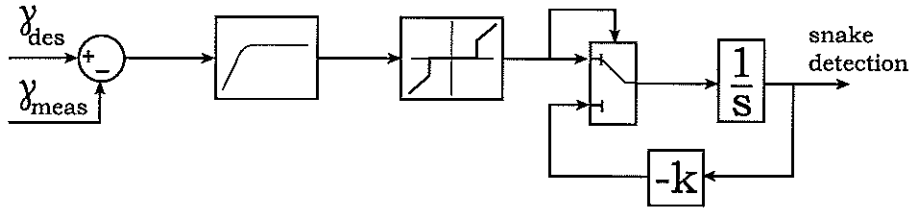

Figure 4.2: Block diagram of the snake detection. First is the error put through a high pass filter, and then integrated if it reaches a certain level lim, otherwise a negative feedback is connected to the integrator. The output from the integrator is the snake detection signal.

This snake detection signal is then used to decrease the controllers dead zone, allowing the controller to interact earlier and prevent the car and trailer from unstable behavior. A block diagram of the whole implementation can be seen in figure 4.3.

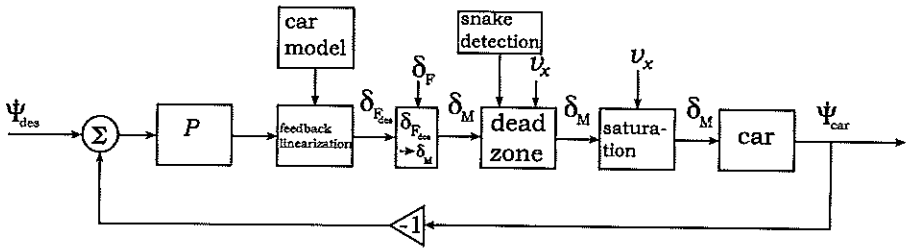

Figure 4.3: Block diagram of the controller implementation. δ_F is the front wheel angle and δ_M is the AFS motor angle. The first block, P, is the linear proportional controller, which is feed with the car's yaw rate error. The linearization feedback block is feed with the linear control signal and f and g from the model block. The model block is feed with signals from the car used to estimate forces. The block that converts the desired front wheel angle to a AFS motor angle is feed with the actual front wheel angle, the desired front wheel angle and the steering wheel angle. The dead zone block and the saturation block is feed with the velocity of the car and the snake detection signal. The output from the saturation block is feed to the AFS system, that actuates the desired AFS motor angle.

4.1.4 Sliding Gain

In blocks with speed dependence sliding gain is used. This is implemented using a lookup table with interpolation. An example can be seen in figure 4.4, where there are given y-values at $v = \{30, 70, 120\}$ and all other y-values are interpolated. Outside the table the output holds the end point values.

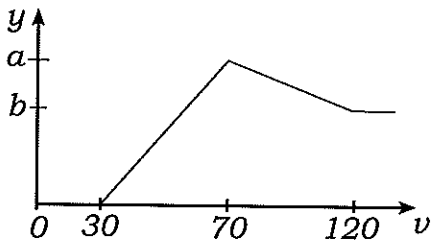

Figure 4.4: Input output graph of a lookup table. v is input and y is output.

4.2 Controller Validation

The controller was validated at Bosch's test track in Boxberg, Germany. The trailer was loaded with maximum allowed load, around 1000 kg, and the center of the load placed over the trailer axle. The weight of the car was around 1800 kg, so this was an instable setup.

The result is shown in the figures 4.5 and 4.6. This clearly shows that the controller works as desired. The driver feels safe driving with the controller turned on, unlike driving in these high speeds without the controller.

The oscillations in figure 4.5 are the oscillations known as snake behavior. The high speed seems to make the car over steered, why small movements on the steering wheel is enough to make the car and trailer oscillate.

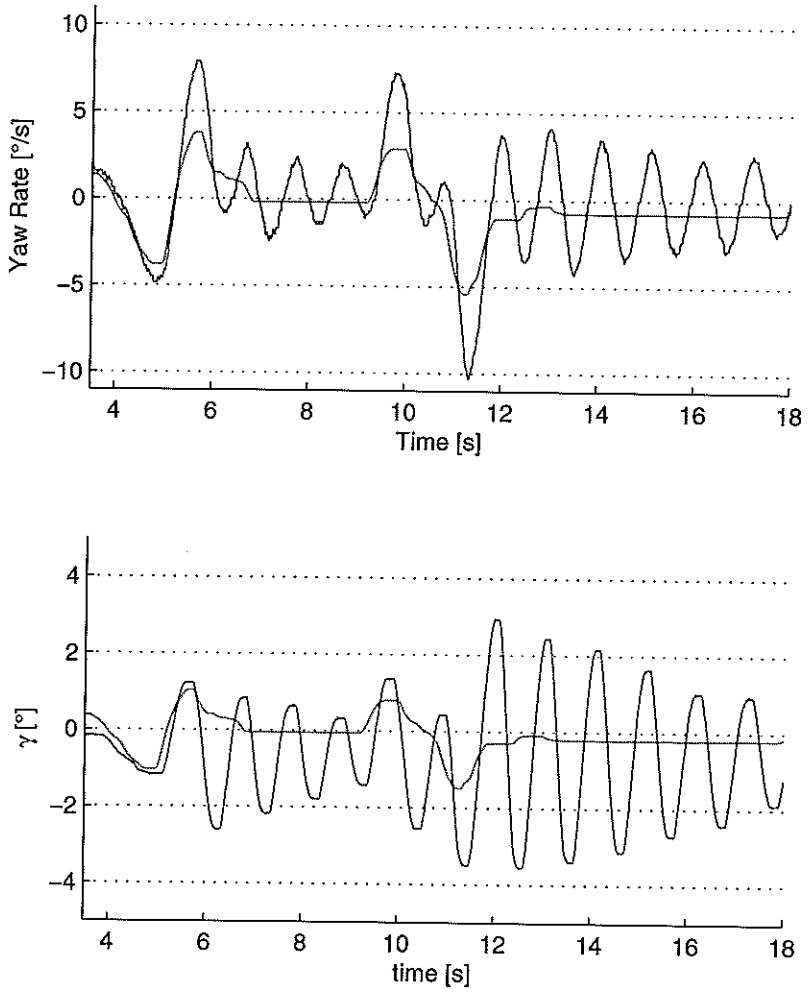

Figure 4.5: Data collected during test drive in 120 km/h without the controller. The red line in the yaw rate and γ graphs is the calculated desired value, the blue line is the measured value. The driving trajectory is a double lane change. After the first lane change the car and trailer starts to oscillate. After the second lane change the oscillations increases but eventually will the oscillations slowly decrease.

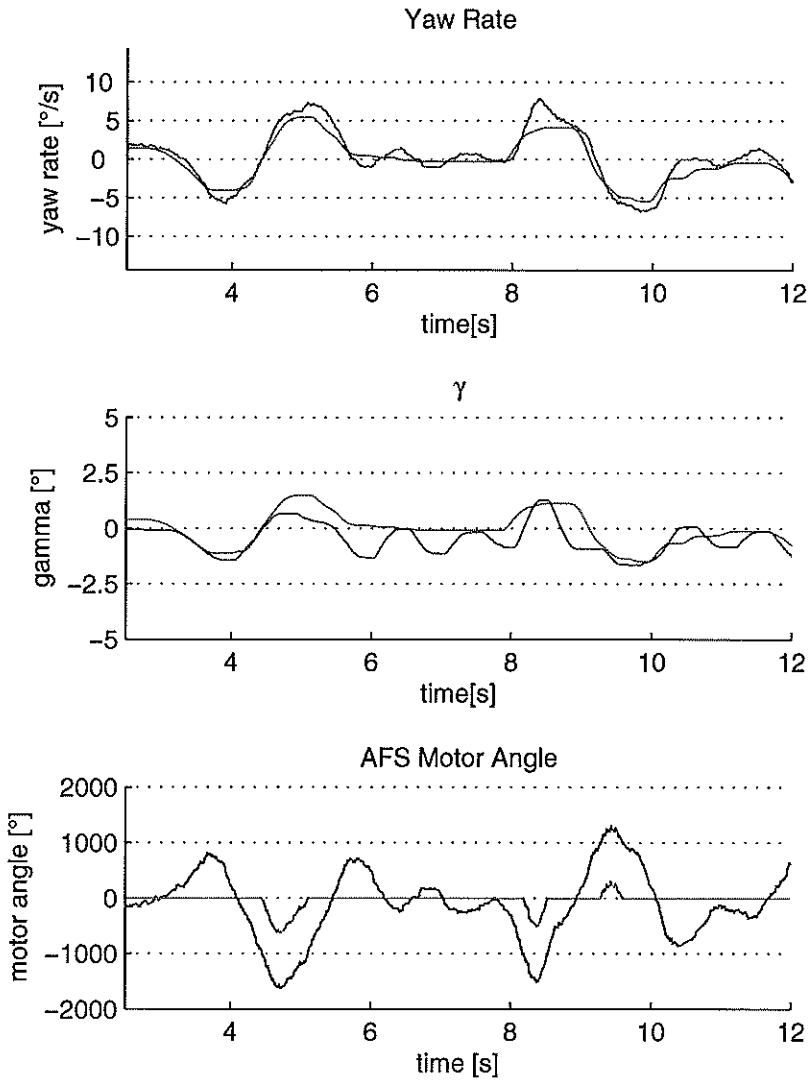

Figure 4.6: Data collected during test drive in 120 km/h with the controller active. The driving trajectory is a double lane change. The red line in the yaw rate and γ graphs is the calculated desired value, the blue line is the measured value. The black line is the desired AFS motor angle from the controller, the green line is the same signal after the dead zone and saturation functions. The controller only intervenes during the lane changes, which clearly is enough to keep the system stable.

Bibliography

[1] H. Hahn, *Rigid Body Dynamics of Mechanisms — 1 Theoretical Basis*, 1 ed. (Springer, 2002), ISBN 3-540-42373-7.

[2] H. Hahn, *Rigid Body Dynamics of Mechanisms — 2 Applicaions*, 1 ed. (Springer Verlag, Berlin, New York, 2003), ISBN 3-540-02237-6.

[3] J. Y. Wong, *Theory of Ground Vehicles* (John Wiley & Sons, 2001), ISBN 0-471-35461-9.

[4] T. N. Gillespie, *Fundamentals of Vehicle Dynamics* (Society of Automotive Engineers, Warrendale, PA, 1992).

[5] P. Brosche, Modellbasierte regelung der quer- und gierdynamik eines fahrzeugs anhand automatischer lenkeingriffe der aktivlenkung, Master's thesis, Fachbereich Maschinenbau, Universität Kassel, Germany, 2005.

[6] A. Andersson, Road-tire friction estimation for afs vehicle control, Master's thesis, Department of Automatic Control, Lunds Institute of Technology, Sweden, 2006.

[7] O. Enqvist, Afs-assisted trailer reversing, Master's thesis, Division of Automatic Control,Department of Electrical Engineering,Linköpings universitet,Sweden, 2006.

[8] J.-J. E. Slotine and W. Li, *Applied Nonlinear Control*, 1 ed. (Prentice-Hall, 1991), ISBN 0-13-040890-5.

[9] K. J. Åström and B. Wittenmark, *Computer-controlled systems: theory and design (2nd ed.)* (Prentice-Hall, Inc., Upper Saddle River, NJ, USA, 1990).

Appendix A

Derivations

A.1 The DE matrix

The DE matrix is the right hand side matrix in (2.35). The left hand side of equation (2.35) can be written as

$$\dot{v} = \begin{pmatrix} \ddot{x} \\ \ddot{y} \\ \ddot{\psi}_1 \\ \ddot{\psi}_2 \end{pmatrix} \tag{A.1}$$

where the different variables are defined in section 2.5.1.

A.1.1 The DE matrix's denominator

There is a special interest in the denominator of the DE matrix because when the denominator equals zero there will be division by zero, which will make the model behavior undefined and not valid. The DE matrix has the denominator

$$\begin{aligned} &[(2m_2^2 + 4m_1m_2 + 2m_1^2)J1 \\ &\quad + (2l_3^2 + 4l_2l_3 + 2l_2^2)m_1m_2^2 \\ &\quad + (2l_3^2 + 4l_2l_3 + 2l_2^2)m_1^2m_2]J_2 \\ &+ (2l_4^2m_1m_2^2 + 2l_4^2m_1^2m_2)J_1 \\ &+ (-l_3^2 - 2l_2l_3 - l_2^2)l_4^2m_1^2m_2^2cos(2\psi_2 - 2\psi_1) \\ &+ (l_3^2 + 2l_2l_3 + l_2^2)l_4^2m_1^2m_2^2 \end{aligned} \tag{A.2}$$

that can be written as

$$\begin{aligned} &(2(m_1 + m_2)^2J1 + 2(l_2 + l_3)^2m_1m_2^2 + 2(l_2 + l_3)m_1^2m_2)J_2 \\ &+ 2l_4^2(m_1m_2^2 + m_1^2m_2)J_1 \\ &- (l_2 + l_3)^2l_4^2m_1^2m_2^2cos2(\psi_2 - \psi_1) \\ &+ (l_2 + l_3)^2l_4^2m_1^2m_2^2 \end{aligned} \tag{A.3}$$

or

$$\begin{aligned} & 2J_2\left(J_1(m_1+m_2)^2+m_1m_2(m_1+m_2)(l_2+l_3)^2\right) \\ & +2J_1l_4^2\left(m_1m_2(m_1+m_2)\right) \\ & +\left(\left(l_2+l_3\right)l_4m_1m_2\right)^2\left(1-\cos(2(\psi_2-\psi_1))\right) \end{aligned} \tag{A.4}$$

or

$$\begin{aligned} & (m_1+m_2)\left[2J_2\left(J_1(m_1+m_2)+m_1m_2(l_2+l_3)^2\right)+2J_1l_4^2m_1m_2\right] \\ & +\left[\left(l_2+l_3\right)l_4m_1m_2\right]^2\left[1-\cos 2(\psi_2-\psi_1)\right] \end{aligned} \tag{A.5}$$

or in a different trigonometric way as

$$\begin{aligned} & (m_1+m_2)\left(2J_2\left[J_1(m_1+m_2)+m_1m_2(l_2+l_3)^2\right]+2J_1l_4^2m_1m_2\right) \\ & +\left[\left(l_2+l_3\right)l_4m_1m_2\right]^2\left(1+\sin^2(\psi_2-\psi_1)-\cos^2(\psi_2-\psi_1)\right) \end{aligned} \tag{A.6}$$

A.1.2 The Different Elements in the DE Matrix

Here are the two last elements in the DE matrix displayed. The different state space variables are defined in section A.2.

The third element, $\ddot{\psi}_1$, in the DE matrix

$$\begin{aligned} & \Big(\big[\cos(x_7-x_5)(m_1m_2+m_1^2)2c_3(l_3+l_2)z_8 \\ & +m_1m_2 2c_2z_7(l_2-l_3)+2c_2(l_2m_1^2-l_3m_2^2)z_7 \\ & +\sin(x_7-x_5)(l_4m_1m_2(m_1+m_2)x_8^2-(m_1m_2+m_1^2)(z_5+z_3))2(l_3+l_2) \\ & +\sin(u)(m_1m_2(l_3+l_2+2l_1)+m_2^2(l_3+l_2+l_1)+l_1m_1^2)2z_1\big]J_2 \\ & +\cos(x_7-x_5)l_4l_5m_1m_2(m_1+m_2)(-l_3-l_2)2c_3z_8 \\ & +l_4^2m_1m_2^2(\cos(2x_7-2x_5)(l_3+l_2)+(l_2-l_3))c_2z_7 \\ & +2c_2l_2l_4^2m_1^2m_2z_7 \\ & +\sin(x_7-x_5)2m_1^2l_4^2m_2(-(z_5+z_3)+l_4m_2x_8^2)(l_3+l_2) \\ & +\sin(2x_7-2x_5)l_4^2m_2^2m_1(l_3+l_2)((z_4+z_2)+(l_3+l_2)m_1x_6^2) \\ & +\sin(u)l_4^2m_1m_2(m_2(l_3+l_2+2l_1)+2l_1m_1)z_1 \\ & -l_4^2m_1m_2^2\sin(2x_7-2x_5-u)(-l_3-l_2)z_1 \\ & +(\cos(u)2c_1(-l_1m_1^2-m_2^2(l_3+l_2+l_1)-m_1m_2(l_3+l_2+2l_1))J_2 \\ & +\cos(u)m_1m_2l_4^2c_1(m_2(-l_3-l_2-2l_1)-2l_1m_1) \\ & +l_4^2m_1m_2^2\cos(2x_7-2x_5-u)c1(l_3+l_2))(z_6) \\ & +(-\cos(u)2c_1(-l_1m_1^2-m_2^2(l_3+l_2+l_1)-m_1m_2(l_3+l_2+2l_1))J_2 \\ & -\cos(u)m_1m_2l_4^2c_1(-m_2(l_3+l_2+2l_1)-2l_1m_1) \\ & -l_4^2m_1m_2^2\cos(2x_7-2x_5-u)c1(l_3+l_2))(u)) \end{aligned}$$

$$\begin{aligned} & (2(m_2+m_1)((m_2+m_1)J_1+m_1m_2(l_3+l_2)^2)J_2 \\ & +2l_4^2m_1m_2(m_2+m_1)J_1 \\ & +(l_3+l_2)^2l_4^2m_1^2m_2^2(1-\cos(2x_7-2x_5))) \end{aligned} \tag{A.7}$$

4th element, $\ddot{\psi}_2$, in the DE matrix

$$
\begin{aligned}
&([2c_3(m_1m_2(2l_5+l_4)+m_1^2(l_5+l_4)+l_5m_2^2)z_8\\
&\quad-\cos(x_7-x_5)2c_2l_4m_2(m_2+m_1)z_7\\
&\quad-\sin(x_7-x_5)(2l_4m_2(m_2+m_1)(z_4+z_2)+2(l_3+l_2)l_4m_1m_2(m_2+m_1)x_6^2)\\
&\quad-\sin(x_7-x_5-u)2l_4m_2(m_2+m_1)z_1]J_1\\
&\quad+m_1^2m_2c_3(l_3+l_2)^2(2l_5+l_4)z_8\\
&\quad+2l_5m_1m_2^2c_3(l_3+l_2)^2z_8\\
&\quad-l_4m_1^2m_2\cos(2x_7-2x_5)c_3(l_3+l_2)^2z_8\\
&\quad+\cos(x_7-x_5)2l_4m_1m_2l_2c_2(-l_3-l_2)(m_1+m_2)z_7\\
&\quad+\sin(2x_7-2x_5)(l_3+l_2)^2m_1^2m_2l_4((z_5+z_3)-l_4m_2x_8^2)\\
&\quad+\sin(x_7-x_5)m_1m_2^2l_4(l_3+l_2)^2((-z_4-z_2)-(l_3+l_2)m_1x_6^2)\\
&\quad-\sin(x_7-x_5-u)l_4m_1m_2(l_3+l_2)(m_2(-l_1+l_3+l_2)-m_1l_1)z_1\\
&\quad-\sin(x_7-x_5+u)l_4m_1m_2(l_3+l_2)(m_2(l_1+l_2+l_3)+m_1l_1)z_1\\
&\quad+\cos(x_7-x_5+u)(l_3+l_2)c_1l_4m_1m_2(m_2(l_3+l_2+l_1)+m_1l_1)z_6\\
&\quad+\cos(x_7-x_5-u)l_4m_1m_2c_1(l_3+l_2)(m_2(l_1-l_3-l_2)+m_1l_1)z_6\\
&\quad-J_1\cos(x_7-x_5-u)2c_1l_4m_2(m_2+m_1)z_6\\
&\quad+[-\cos(x_7-x_5+u)(l_3+l_2)c_1l_4m_1m_2(m_2(l_3+l_2+l_1)+m_1l_1)\\
&\quad-\cos(x_7-x_5-u)l_4m_1m_2c_1(l_3+l_2)(m_2(l_1-l_3-l_2)+m_1l_1)\\
&\quad+J_1\cos(x_7-x_5-u)2c_1l_4m_2(m_2+m_1)](u))\\
&\hline
&\quad(2(m_2+m_1)((m_2+m_1)J_1+m_1m_2(l_3+l_2)^2)J_2\\
&\qquad+2l_4^2m_1m_2(m_2+m_1)J_1\\
&\qquad+(l_3+l_2)^2l_4^2m_1^2m_2^2(1-\cos(2x_7-2x_5)))
\end{aligned}
\tag{A.8}
$$

A.2 State Space Variables

Observe that these x_i are the model state variables, and are not to be confused with car or trailer position x_i^R.

Here are all the state space variables listed to clarify any uncertainty.

$$
\begin{aligned}
u &= \delta_F \\
\begin{cases} x_1 &= x^R_{P_1O} \\ x_2 &= v^R_{x_1} (= \dot{x}^R_1) \\ x_3 &= y^R_{P_1O} \\ x_4 &= v^R_{y_1} \\ x_5 &= \psi_1 \\ x_6 &= \dot{\psi}_1 \\ x_7 &= \psi_2 \\ x_8 &= \dot{\psi}_2 \end{cases} \\
\begin{cases} \dot{x}_1 &= x_2 \\ \dot{x}_2 &= \dot{v}[1] \\ \dot{x}_3 &= x_4 \\ \dot{x}_4 &= \dot{v}[2] \\ \dot{x}_5 &= x_6 \\ \dot{x}_6 &= \dot{v}[3] \\ \dot{x}_7 &= x_8 \\ \dot{x}_8 &= \dot{v}[4] \end{cases} \\
\begin{cases} z_1 &= f_{lf} \\ z_2 &= f_{lr} \\ z_3 &= f_{lt} \\ z_4 &= f_{airc} \\ z_5 &= f_{airt} \\ z_6 &= \alpha_F \\ z_7 &= \alpha_R \\ z_8 &= \alpha_T \end{cases}
\end{aligned}
\tag{A.9}
$$

Here f_{lf} is the force acting in longitudinal direction on the front wheel, f_{lr} is acting on the rear wheel and f_{lt} is acting on the trailer wheel. f_{airc} and f_{airt} are the air resistance force acting on the car and trailer respectively. z_6, z_7 and z_8 are the slip angles for the different wheels.

A.2.1 The DEs written with State Space Variables

With the state space variables defined it is possible to rewrite the DEs.

$$
\begin{cases}
\dot{x}_1 &= x_2 \\
\dot{x}_2 &= f_1(x,z,u) + g_1(x,z,u) \cdot u \\
\dot{x}_3 &= x_4 \\
\dot{x}_4 &= f_2(x,z,u) + g_2(x,z,u) \cdot u \\
\dot{x}_5 &= x_6 \\
\dot{x}_6 &= f_3(x,z,u) + g_3(x,z,u) \cdot u \\
\dot{x}_7 &= x_8 \\
\dot{x}_8 &= f_4(x,z,u) + g_4(x,z,u) \cdot u
\end{cases}
\tag{A.10}
$$

and if only the state space variables that are used are considered it can be written as

$$\begin{cases} \dot{x}_1 &= x_2 \\ \dot{x}_2 &= f_1(x,z,u) + g_1(x,z,u)\cdot u \\ \dot{x}_3 &= x_4 \\ \dot{x}_4 &= f_2(x,z,u) + g_2(x,z,u)\cdot u \\ \dot{x}_5 &= x_6 \\ \dot{x}_6 &= f_3(x_5 \ldots x_8,z,u) + g_3(x_5,x_7,u)\cdot u \\ \dot{x}_7 &= x_8 \\ \dot{x}_8 &= f_4(x_5 \ldots x_8,z,u) + g_4(x,z,u)\cdot u \end{cases} \tag{A.11}$$

A.3 DAE Projection Matrices

Here are the different matrices used in the DAE projection displayed.

$$\begin{aligned} p_{\text{ind}} &= P_{r\text{ind}} \cdot p \\ &= \begin{pmatrix} 1 & 0 & 0 & 0 & 0 & 0 \\ 0 & 1 & 0 & 0 & 0 & 0 \\ 0 & 0 & 1 & 0 & 0 & 0 \\ 0 & 0 & 0 & 0 & 0 & 1 \end{pmatrix} \cdot \begin{pmatrix} x^R_{P_1O} \\ y^R_{P_1O} \\ \psi_1 \\ x^R_{P_2O} \\ y^R_{P_2O} \\ \psi_2 \end{pmatrix} \\ p_{\text{dep}} &= P_{r\text{dep}} \cdot p \\ &= \begin{pmatrix} 0 & 0 & 0 & 1 & 0 & 0 \\ 0 & 0 & 0 & 0 & 1 & 0 \end{pmatrix} \cdot \begin{pmatrix} x^R_{P_1O} \\ y^R_{P_1O} \\ \psi_1 \\ x^R_{P_2O} \\ y^R_{P_2O} \\ \psi_2 \end{pmatrix}. \end{aligned} \tag{A.12}$$

With the information about the dependent variables from the constraints equations (2.20) yields

$$p_{dep} = \begin{pmatrix} x^R_{P_2O} \\ y^R_{P_2O} \end{pmatrix} = \begin{pmatrix} x^R_{P_1O} - (l_3 + l_2)\cdot\cos\psi_1 - l_4\cdot\cos\psi_2 \\ y^R_{P_1O} - (l_3 + l_2)\cdot\sin\psi_1 - l_4\cdot\sin\psi_2 \end{pmatrix}. \tag{A.13}$$

Together with

$$p_{\text{ind}} = \begin{pmatrix} x^R_{P_1O} \\ y^R_{P_1O} \\ \psi_1 \\ \psi_2 \end{pmatrix} \tag{A.14}$$

yields these equations the explicit constraints position equations

$$p = h(p_{\text{ind}}) = \begin{pmatrix} x^R_{P_1O} \\ y^R_{P_1O} \\ \psi_1 \\ x^R_{P_1O} - (l_3 + l_2) \cdot \cos\psi_1 - l_4 \cdot \cos\psi_2 \\ y^R_{P_1O} - (l_3 + l_2) \cdot \sin\psi_1 - l_4 \cdot \sin\psi_2 \\ \psi_2 \end{pmatrix}. \tag{A.15}$$

Further is

$$\begin{aligned} h_{p_{\text{ind}}}(p_{\text{ind}}) &= \frac{\partial h(p_{\text{ind}})}{\partial p_{\text{ind}}} = \\ &= \begin{pmatrix} 1 & 0 & 0 & 0 \\ 0 & 1 & 0 & 0 \\ 0 & 0 & 1 & 0 \\ 1 & 0 & (l_3 + l_2) \cdot \sin\psi_1 & l_4 \cdot \sin\psi_2 \\ 0 & 1 & -(l_3 + l_2) \cdot \cos\psi_1 & -l_4 \cdot \cos\psi_2 \\ 0 & 0 & 0 & 1 \end{pmatrix} \end{aligned} \tag{A.16}$$

and the time derivative of the independent position vector

$$\dot{p}_{\text{ind}} = v_{\text{ind}} = \begin{pmatrix} \dot{x}^R_{P_1O} \\ \dot{y}^R_{P_1O} \\ \dot{\psi}_1 \\ \dot{\psi}_2 \end{pmatrix} \tag{A.17}$$

and

$$\begin{aligned} T_{\text{ind}}(p_{\text{ind}}) &= I_4 \\ T &= I_6. \end{aligned} \tag{A.18}$$

The global projector is defined as

$$J_v = T^{-1} \cdot h_{p_{\text{ind}}} \cdot T_{\text{ind}} \tag{A.19}$$

with the time derivative

$$\dot{J}_v = \dot{h}_{p_{\text{ind}}}(p_{\text{ind}}) = \begin{pmatrix} 0 & 0 & 0 & 0 \\ 0 & 0 & 0 & 0 \\ 0 & 0 & 0 & 0 \\ 0 & 0 & (l_3 + l_2) \cdot \cos\psi_1 \cdot \dot{\psi}_1 & l_4 \cdot \cos\psi_2 \cdot \dot{\psi}_2 \\ 0 & 0 & (l_3 + l_2) \cdot \sin\psi_1 \cdot \dot{\psi}_1 & l_4 \cdot \sin\psi_2 \cdot \dot{\psi}_2 \\ 0 & 0 & 0 & 0 \end{pmatrix} \tag{A.20}$$

and the following matrices are defined

$$M_{\text{ind}} = h^T_{p_{\text{ind}}} \cdot M \cdot h_{p_{\text{ind}}} = \tag{A.21}$$

$$\left(\begin{array}{cc|cc} m_1+m_2 & 0 & & \\ 0 & m_1+m_2 & & \\ (l_2+l_3)\cdot m_2\cdot\sin\psi_1 & -(l_2+l_3)\cdot m_2\cdot\cos\psi_1 & & \\ l_4\cdot m_2\cdot\sin\psi_2 & -l_4\cdot m_2\cdot\cos\psi_2 & & \end{array}\right.$$
$$\left.\begin{array}{cc} (l_2+l_3)\cdot m_2\cdot\sin\psi_1 & l_4\cdot m_2\cdot\sin\psi_2 \\ -(l_2+l_3)\cdot m_2\cdot\cos\psi_1 & -l_4\cdot m_2\cdot\cos\psi_2 \\ J_1+(l_2+l_3)^2\cdot m_2 & (l_2+l_3)\cdot l_4\cdot m_2\cdot\cos(\psi_1+\psi_2) \\ (l_2+l_3)\cdot l_4\cdot m_2\cdot\cos(\psi_1+\psi_2) & J_2+l_4^2\cdot m_2 \end{array}\right) \tag{A.22}$$

and

$$f_{\text{ind}} = h_{p_{\text{ind}}}^T \cdot f - h_{p_{\text{ind}}}^T \cdot M \cdot \dot{h}_{p_{\text{ind}}} \cdot v_{\text{ind}} \tag{A.23}$$

where

$$h_{p_{\text{ind}}}^T \cdot f = \begin{pmatrix} \sum F_{x1}^R + \sum F_{x2}^R \\ \sum F_{y1}^R + \sum F_{y2}^R \\ \sum M_1^{L_1} + (l_2+l_3)\cdot\sin\psi_1\cdot\sum F_{x2}^R - (l_2+l_3)\cdot\cos\psi_1\cdot\sum F_{y2}^R \\ \sum M_2^{L_2} + l_4\cdot\sin\psi_2\cdot\sum F_{x2}^R - l_4\cdot\cos\psi_2\cdot\sum F_{y2}^R \end{pmatrix} \tag{A.24}$$

and

$$h_{p_{\text{ind}}}^T \cdot M \cdot \dot{h}_{p_{\text{ind}}} \cdot v = \tag{A.25}$$

$$\begin{pmatrix} (l_2+l_3)\cdot m_2\cdot\cos\psi_1\cdot\dot{\psi}_1^2 + l_4\cdot m_2\cdot\cos\psi_2\cdot\dot{\psi}_2^2 \\ (l_2+l_3)\cdot m_2\cdot\sin\psi_1\cdot\dot{\psi}_1^2 + l_4\cdot m_2\cdot\sin\psi_2\cdot\dot{\psi}_2^2 \\ -(l_2+l_3)\cdot l_4\cdot m_2\cdot\sin(\psi_2-\psi_1)\cdot\dot{\psi}_2^2 \\ (l_2+l_3)\cdot l_4\cdot m_2\cdot\sin(\psi_2-\psi_1)\cdot\dot{\psi}_1^2 \end{pmatrix} \tag{A.26}$$

and

$$q_{G_{\text{ind}}}(p_{\text{ind}}, v_{\text{ind}}) = 0.$$

With these matrix definitions the DEs are given according to the following matrix relationship

$$
\begin{pmatrix}
m_1+m_2 & 0 & | & (l_2+l_3)\cdot m_2\cdot\sin\psi_1 & l_4\cdot m_2\cdot\sin\psi_2 \\
0 & m_1+m_2 & | & -(l_2+l_3)\cdot m_2\cdot\cos\psi_1 & -l_4\cdot m_2\cdot\cos\psi_2 \\
(l_2+l_3)\cdot m_2\cdot\sin\psi_1 & -(l_2+l_3)\cdot m_2\cdot\cos\psi_1 & | & J_1+(l_2+l_3)^2\cdot m_2 & (l_2+l_3)\cdot l_4\cdot m_2\cdot\cos(\psi_1+\psi_2) \\
l_4\cdot m_2\cdot\sin\psi_2 & -l_4\cdot m_2\cdot\cos\psi_2 & | & (l_2+l_3)\cdot l_4\cdot m_2\cdot\cos(\psi_1+\psi_2) & J_2+l_4^2\cdot m_2
\end{pmatrix}
\cdot
\begin{pmatrix}
{}^R\ddot{x}^R_{P_1O} \\ {}^R\ddot{y}^R_{P_1O} \\ \ddot{\psi}_1 \\ \ddot{\psi}_2
\end{pmatrix} =
$$

$$
\begin{pmatrix}
\sum F^R_{x1}+\sum F^R_{x2} \\
\sum F^R_{y1}+\sum F^R_{y2} \\
\sum M^{L_1}_1+(l_2+l_3)\cdot\sin\psi_1\cdot\sum F^R_{x2}-(l_2+l_3)\cdot\cos\psi_1\cdot\sum F^R_{y2} \\
\sum M^{L_2}_2+l_4\cdot\sin\psi_2\cdot\sum F^R_{x2}-l_4\cdot\cos\psi_2\cdot\sum F^R_{y2}
\end{pmatrix}
-
\begin{pmatrix}
(l_2+l_3)\cdot m_2\cdot\cos\psi_1\cdot\dot{\psi}_1^2+l_4\cdot m_2\cdot\cos\psi_2\cdot\dot{\psi}_2^2 \\
(l_2+l_3)\cdot m_2\cdot\sin\psi_1\cdot\dot{\psi}_1^2+l_4\cdot m_2\cdot\sin\psi_2\cdot\dot{\psi}_2^2 \\
-(l_2+l_3)\cdot l_4\cdot m_2\cdot\sin(\psi_2-\psi_1)\cdot\dot{\psi}_2^2 \\
(l_2+l_3)\cdot l_4\cdot m_2\cdot\sin(\psi_2-\psi_1)\cdot\dot{\psi}_1^2
\end{pmatrix}
$$

A.4 Axle Load of Trailer and Car

Let the forces, heights and lengths be defined according to figure 2.9. Then the torque equations around the contact surface for each wheel and the torque equation around the towing hook can be written as

$$
\begin{aligned}
M_{rear\ wheel} = &- m_1\cdot g\cdot l_2 - f_{airc}\cdot h_{airc} + N_F\cdot(l_1+l_2) \\
&- F_{Th}\cdot l_3 - F_{Tl}\cdot h_t - F_{axc}\cdot h_{cc} = 0
\end{aligned} \tag{A.27a}
$$

$$
\begin{aligned}
M_{front\ wheel} = &\ m_1\cdot g\cdot l_1 - f_{airc}\cdot h_{airc} - N_R\cdot(l_1+l_2) \\
&- F_{Th}\cdot(l_1+l_2+l_3) - F_{Tl}\cdot h_t - F_{axc}\cdot h_{cc} = 0
\end{aligned} \tag{A.27b}
$$

$$
\begin{aligned}
M_{trailer\ wheel} = &- m_2\cdot g\cdot l_5 - f_{airt}\cdot h_{airt} + F_{Th}\cdot(l_4+l_5) \\
&+ F_{Tl}\cdot h_t - F_{axt}\cdot h_{ct} = 0
\end{aligned} \tag{A.27c}
$$

$$
\begin{aligned}
M_{trailer\ hook} = &\ m_2\cdot g\cdot l_4 - f_{airt}\cdot(h_{airt}-h_t) - N_t\cdot(l_4+l_5) \\
&+ f_{lt}\cdot h_t - F_{axt}\cdot(h_{ct}-h_t) = 0
\end{aligned} \tag{A.27d}
$$

where

$$
F_{Tl} = F_{axt} + F_{airt} + f_{lt}. \tag{A.27e}
$$

From equation (A.27a) to (A.27d) is it now possible to derive the normal forces for each wheel, N_F, N_R and N_T,

$$F_{Th} = \frac{m_2 \cdot g \cdot l_5 + f_{airt} \cdot h_{airt} - F_{Tl} \cdot h_t + F_{axt} \cdot h_{ct}}{l_4 + l_5} \tag{A.28a}$$

$$N_F = \frac{m_1 \cdot g \cdot l_2 + f_{airc} \cdot h_{airc} + F_{Th} \cdot l_3 + F_{Tl} \cdot h_t + F_{axc} \cdot h_{cc}}{l_1 + l_2} \tag{A.28b}$$

$$N_R = \frac{m_1 \cdot g \cdot l_1 - f_{airc} \cdot h_{airc} - F_{Th} \cdot (l_1 + l_2 + l_3) - F_{Tl} \cdot h_t - F_{axc} \cdot h_{cc}}{l_1 + l_2} \tag{A.28c}$$

$$N_T = \frac{m_2 \cdot g \cdot l_4 - f_{airt} \cdot (h_{airt} - h_t) + f_{lt} \cdot h_t - F_{axt} \cdot (h_{ct} - h_t)}{l_4 + l_5} \tag{A.28d}$$